QUALITATIVE HEALTH MONITORING AND INCIPIENT DAMAGE INSPECTION/EVALUATION

by

John W. Ayres III

Thesis submitted to the faculty of the
Virginia Polytechnic Institute and State University
in partial fulfillment of the requirements for the degree of
Master of Science
in
Mechanical Engineering

APPROVED:

Dr. Craig A. Rogers, Chairman

Dr. Frederic Lalande

Dr. Harry H. Robertshaw

May, 1996
Blacksburg, Virginia

Key Words: Damage Detection, Qualitative, Smart Structures, Impedance

c.2

LD
5655
V855
1996
A947
c.2

Qualitative Health Monitoring and Incipient Damage Inspection/Evaluation

by

John W. Ayres III

Dr. Craig A. Rogers, Chairman

Mechanical Engineering

(ABSTRACT)

Real-time structural integrity monitoring is a concept that is becoming a reality in the engineering community. It will soon be possible for a structure to warn the user when its own structural integrity has been altered.

A qualitative impedance-based health monitoring technique, which can be implemented for real-time damage evaluation of complex structures, is investigated. The basic principle of the technique is to monitor the structure's mechanical impedance which will be changed with the presence of damage. The mechanical impedance variations are monitored by measuring the electrical impedance of a bonded piezoelectric actuator/sensor (PZT). This mechanical-electrical impedance relation is due to the electro-mechanical coupling property of piezoelectric materials. This health monitoring technique can be easily adapted to existing structures, since only a small non-intrusive PZT patch is needed. This impedance-based method operates at high frequencies (generally above 100kHz), which enables it to detect incipient type damage in a localized region. The localized sensing region offers the advantage of not being affected by normal operating conditions or by changing boundary conditions. In this thesis, a complete theoretical background on the impedance-based technique is derived. Then, the technique is applied successfully to a variety of case studies; such as composite patch repair, aircraft structures, precision parts, and civil infrastructure. By simplifying the impedance measurement interpretation through a simple scalar damage metric, the real-time implementation of the impedance-based technique has been proven feasible.

ACKNOWLEDGMENTS

I would like to express my deepest gratitude to Dr. Craig Rogers for this wonderful opportunity. Not only have you been an advisor to me for this thesis, but also a friend. I thank you for the many discussions we had over the past couple of years. Technical or not, I always enjoyed a conversation with you. I would also like to thank my committee members, Dr. Frederic Lalande and Dr. Harry Robertshaw. Dr. Lalande I thank for being there when I needed help or direction especially in the preparation of this thesis, and Dr. Robertshaw for being a friend. I will never forget our NOC trip where we almost froze.

I would also like to thank the staff at the Center for Intelligent Material Systems and Structures. Special thanks to the graphics department for the unconditional use of their equipment, and Beth and Stacie for always answering questions with a smile.

Finally, I would like to thank my friends that have always stood by me. I thank Rob for introducing me to the love of a lifetime. Rob, I can never thank you enough! I thank Susan for the time that we spent together and for the time that is yet to come. Last, but certainly not least, I thank my parents. It is their love an support that fueled my desire to learn. I thank my mom for constantly pushing me and I thank my dad for being my best friend.

TABLE OF CONTENTS

1 INTRODUCTION

1.1 Motivation 1

1.1.1 Intelligent Material Systems 1

1.1.2 Health Monitoring 3

1.1.3 Qualitative vs. Quantitative 5

1.2 Objectives 10

1.3 Impedance-Based Health Monitoring 10

1.4 Applications 12

1.5 Thesis Organization 13

2 THEORY

Theory 14

2.1 Impedance-Based Health Monitoring 14

2.1.1 Mechanical Impedance 14

2.2 Dynamic Analysis Using Impedance 17

2.3 Characteristics of Piezoelectric Material 19

2.4 Coupled Electromechanical Modeling 21

2.5 Coupled Electromechanical Impedance 27

3 EXPERIMENTAL APPLICATIONS AND RESULTS

Experimental Results 29

3.1 Damage Metric Definition 29

3.2 Composite Patch Repair 30

3.3 Complex Precision Parts 40

3.4 Space-Bay Truss 48

3.5 Aircraft Structures 53

3.6 Massive Civil Infrastructure 61

4 CONCLUSIONS

4.1 Discussion 70

4.2 Future Issues..... 71

4.3 Conclusions 71

REFERENCES 73

VITA 75

LIST OF FIGURES

1.1 Impedance-Based Health Monitoring can Replace Routine Maintenance Inspections 4

1.2 Benefits of Qualitative and Quantitative Damage Detection 8

1.3 Example of Incipient Damage 9

1.4 Catastrophic Failure of a Structure that Could Have Been Prevented had it Been Detected Early 12

2.1 Spring driven by a PZT actuator 15

2.2 The Mechanical Impedance of a Structure is Dependent on the Excitation Frequency of the System 16

2.3 The Mechanical Impedance of a Single-Degree-of-Freedom Spring-Mass-Damper System is Dependent on the Driving Frequency 17

2.4 Schematic Illustration of a PZT Lumped Parameter System 21

2.5 HP Impedance Analyzer 28

3.1 Geometry of Plate Test Specimen Received From E-Systems 31

3.2 Large Frequency Interval Effect of De-Bonding 34

3.3 Small Frequency Interval Effect of De-Bonding 35

3.4 Geometry of Dog-bone Specimen 36

3.5 Effect of Crack Growth on the Impedance of a Dog-bone Specimen 37
3.6 Effect of Crack Growth on the Impedance of a Dog-bone Specimen 38
3.7 Qualitative Comparison of the Different Stages of De-Bonding 39
3.8 Precision Gears With Bonded PZT Actuator/Sensor 41
3.9 Progressive Stages of Gear Tooth Wear 41
3.10 Location of Tooth Bending Cracks on Type 1 Gears 42
3.11 The Impedance-Based Technique Used for Quality Control in Precision Parts 43
3.12 The Effect of Abrasive Gear Wear 44
3.13 The Effect of a 0.18 in. Deep Crack from Simulated Bending Fatigue 45
3.14 The Effect of a 0.05 in. Deep Crack from Simulated Bending Fatigue 46
3.15 Qualitative Comparison of the Different Damage Tests to Precision Gears . 47
3.16 Brussels Space-Bay Truss Structure 49
3.17 Space-Bay Test Set-Up and Instrumentation 49
3.18 Small Variations in the Structural Admittance Due to Local Structural Alterations 50
3.19 The Small Effect of Global or Far-Field Damage on the Sensing Technique 51
3.20 Qualitative Comparison of the Damage to a Space-Truss Structure 52
3.21 The Tail Section of a Piper 601P Aircraft 54
3.22 Close-Up view to the Local Damage Area of the Aircraft 55
3.23 The Smallest Local Structural Alteration Results in a Change in the Admittance Measurements 56
3.24 Larger Structural Alterations Change the Admittance Measurements Significantly 57
3.25 Far-Field Structural Alterations Have Very Little Effect on the Sensing Technique 58
3.26 Normal Operations, Such as Varying the Rudder Position, has Very Little Effect on the Impedance-Based Sensing Technique 59

3.27 Qualitative Comparison of the Damage to the Aircraft 60
3.28 The Bridge Joint Used in the Experiments 62
3.29 Close-Up of the Bridge Joint 62
3.30 The Local Sensing Area is Insensitive to Global Structural Alterations 64
3.31 Small Amounts of Local Damage to Massive Structures Effects the Admittance Measurements 65
3.32 Small Amounts of Local Damage Produces a Vertical Shift in the Admittance Measurements for Massive Structures 66
3.33 Large Amounts of Local Damage has a Large Effect on the Admittance Measurements 67
3.34 Qualitative Comparison for Civil Infrastructure 68

LIST OF TABLES

1.1 Qualitative vs. Quantitative damage detection 9

1.2 Applications of Qualitative damage detection 13

3.1 Frequency intervals 32

NOMENCLATURE

c	Damping coefficient
D_3	Electric displacement
d_{32}	Piezoelectric constant
E	The electric field
$\bar{\varepsilon}_{33}^{T}$	Complex dielectric constant
F	Dynamic interaction force
F(ω)	Force dependent of excitation frequency
h_a	PZT thickness
I	Electric current
i	Defined as $(-1)^{1/2}$
K_A	Spring stiffness
K_D	Dynamic stiffness
K_S	Static stiffness of PZT
l_a	Length of PZT
M	Metric used to qualitatively asset damage
m	Mass
ρ	Density of PZT
S_2	Mechanical strain
$\bar{s}_{22}^{E}$	Complex compliance @ zero electric field
T_2	Mechanical stress

V	Displacement in the y-direction
$\overline{Y}_{22}^{E}$	Complex modulus of the PZT at zero electric field (inverse of the Complex compliance)
Y	Coupled electromechanical admittance
Y(ω)	Frequency dependent admittance
$Y_{i,1}$	Admittance before a structural alteration
$Y_{i,2}$	Admittance after a structural alteration
Y	Coupled electrical mechanical admittance
$\dot{x}(\omega)$	Velocity dependent on frequency
Λ	Free induced displacement
ω_n	Natural frequency
ω	Frequency in Hz.
Z(ω)	Frequency dependent Impedance
Z	Structural mechanical impedance
Z_a	Actuator impedance

CHAPTER 1

INTRODUCTION

This introduction will review some of the basic topics that are discussed in this thesis. This will include a brief discussion of intelligent material systems, qualitative damage detection, and health monitoring which provides the motivation for this work. It will also discuss the relevance of this technique and its applications.

1.1 MOTIVATION

1.1.1 INTELLIGENT MATERIAL SYSTEMS

The term "intelligent material", or "smart system" is fast becoming a common phrase among the engineering community. These terms are used to describe a variety of modern advances in the world of engineering. There is no agreed definition for this intelligent system. However, the most widely used definition follows: "Intelligent material systems, defined from a technology standpoint, are the integration of actuators, sensors, and controls with a material or structural component" (Rogers et al., 1992). This definition describes the compotes that make up a "smart system", but does not state the objective of this extensive area of research. The definition from a science standpoint that attempts to capture a more global definition is stated as: "to create material systems with intelligence

and life features integrated in the microstructure of the material system to reduce mass and energy and produce adaptive functionality" (Rogers et al., 1992). That is, the goal of a material system is to design structures only as strong as need be, and use as little energy as possible over its lifetime. Because the conditions surrounding the world are constantly changing, we need systems that will adapt to these changes. In the natural world (as opposed to the synthetic world) nature adapts to the changing environment expending in the process only the necessary amount of energy needed to complete a certain task. The idea of "Smart Systems" borrows this concept of natural change and adapts it to the scientific world.

According to Baker (1989), the common features that should be included in any definition of smart or intelligent structures are:

Sensors Smart structures have non-intrusive sensors which recognize and measure the intensity of stimulus which could be force-like, displacement-like, thermal, electric, magnetic, chemical, etc.

Actuators Smart structures have non-intrusive actuators to respond to the stimulus.

Control Mechanism Smart structures have the ability to control the response to the stimulus according to a predetermined relationship. The control mechanism must be capable of selecting response if more than one is available.

Time and Nature of Response Smart structures have fast response in relation to stimulus. The system returns to its original state when the stimulus is removed.

1.1.2 HEALTH MONITORING

Today, in the world of engineering, there is a growing interest in the development of real-time damage detection methods. This type of method allows systems and structures to actively monitor their own structural integrity while in operation and throughout the life of the structure. This concept is known as health monitoring. It is a specific type of non-destructive evaluation (NDE). An important requirement on real-time damage detection techniques is that the technique should not be affected by the normal operation of the system or structure. If the real-time NDE technique is affected by normal operation, it can be difficult to distinguish between these changes from those caused by damage. Normal use can be any structural alteration that is not local to the sensing area. This can be a truck crossing a bridge or any normal structural change. The basic premises of real-time health monitoring is to increase the knowledge of the current status of the structure. By having a more detailed history of the structure, it is much easier to assess the current status of the structure. The ultimate goal in health monitoring is to be able to remotely monitor the structures integrity by computer and warn the user when damage is initiated. This can be seen in Fig. 1.1 where a bridge is remotely monitored using this technique. A red light at the damage control panel warns the user of incipient damage at its early stage. Because of this increased knowledge of the current status of the structure, this technique has the potential to replace many routine maintenance inspections.

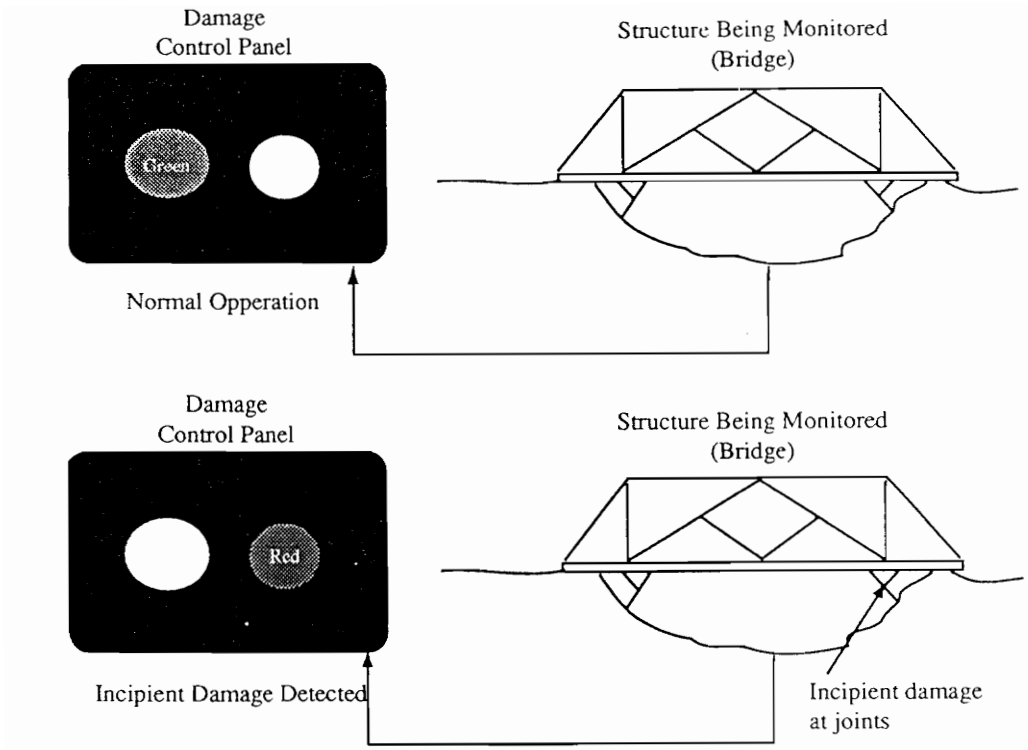

Figure 1.1 Health Monitoring can replace routine maintenance inspections. The structure only needs to be inspected when incipient damage is detected.

1.1.3 QUALITATIVE VS. QUANTITATIVE

Most of the non-destructive evaluation (NDE) techniques currently used are very efficient in detecting the nature, size, and location of structural damage accurately. However, these quantitative techniques, such as ultrasonic scans, X-radiography, and passive thermography, often require direct access to the structure and involves bulky equipment. One common quantitative NDE technique is ultrasonic (A, B, and C scans), which monitors the transducer echoes of the test specimen as a function of the time to detect the presence of defects. This technique is very useful in quantitatively assessing the size and the extent of damage present in the structure. However, it requires a liquid couplet between the ultrasonic transducer and the structure for accurate results. A liquid bath is not very practical, especially in large or remote sensing applications. Liquid jet probes require direct access to the structure and have a very limited sensing area. There are also many NDE techniques that are based on the variation of the structural vibrational properties. Included in this sonic vibration family are: the coin-tap test (Cawley and Adams, 1988), the mechanical impedance method (Cawley, 1987), and the membrane resonance method (Cawley and Theodorakopoulos, 1989). Most of these techniques do not require a liquid coupling, but still require a physical contact between the transducer and the structure. Also, the sensitivity of the sonic vibration methods to small structural changes is limited due to the low operating frequency at a maximum of 30 kHz (Guyott et al., 1986). There are other quantitative NDE methods such as X-radiography, passive thermography, and laser Doppler vibrometry, but they all require direct access to the structure.

These quantitative methods share the common handicap of requiring direct access to the structure and often involve bulky equipment. It is the high level of information given by these quantitative techniques that requires such elaborate equipment. These types of sensing techniques are not practical for use in a real-time application. On the other hand, the qualitative method looks at the damage identification from another perspective: Get a

limited amount of information about the structure with smaller non-intrusive equipment. By being non-intrusive, the sensor will not effect the normal operation of the structure being monitored. Thus, the qualitative technique's configuration makes it more appropriate for real-time NDE applications and makes it easy to adapt to existing complex structures. Such a qualitative sensing technique can reduce the structures down time during inspections and reduce maintenance costs.

Which damage detection method is better: quantitative or qualitative? There is not a clear answer to this question. It depends on the circumstances. If the structure is already damaged, then a high resolution of a quantitative method would be the best choice to determine the extent of the damage. However, if damage is not present in the structure, a qualitative method capable of detecting damage at an early stage would be more appropriate. Figure 1.2 presents two damage outputs from a qualitative technique (top) and a quantitative technique (bottom). In the top graph the presents of damage to the composite beam has been detected. It shows up as a large percent damage in a simple bar graph. Normal operation is below 5% damage; thus the graph revels the presents of damage by the high damage index (percent damage). This technique does not tell us anything about the damage, only that the beam is damaged. The bottom graph is a quantitative, high frequency laser scan of the damaged section in the composite beam. It revels the extent and the type of damage, in this case a delimitation of the composite. Each method has benefits depending on the circumstances. In most cases, a qualitative technique will detect the damage at an early stage and minimize the time needed to repair the structure.

It is often better to detect damage before it becomes large enough to inhibit the structure's performance and before it becomes to expensive to repair. A good health monitoring method should be able to detect incipient type damage. This incipient type damage has no significant effect on the structural integrity or the operation of the system

being monitored, but often leads to large damage if not detected at an early stage. The loosening of one bolt in a large structure can be described as incipient damage (Fig. 1.3). Therefore, the objectives of qualitative and quantitative methods are different, and should be used in the appropriate application. Table 1.1 shows some of the comparisons between the qualitative and quantitative methods. Quantitative methods can be used after incipient damage has been detected by qualitative health monitoring. This qualitative method can determine when to use the quantitative inspection techniques. This two stage type of NDE system can greatly reduce the maintenance cost of the structure and reduce the down time from needless inspections. This is due to a better knowledge of the structure's status over its lifetime.

Qualitative Damage Detection

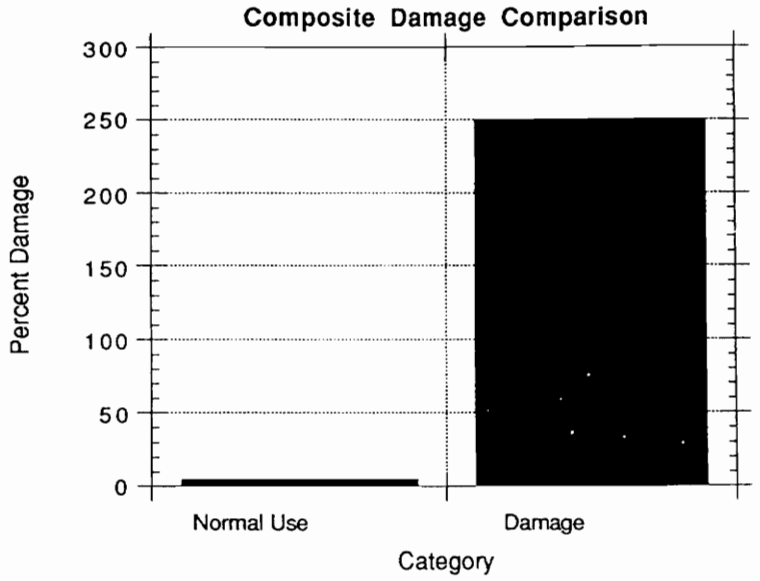

Quantitative Damage Detection

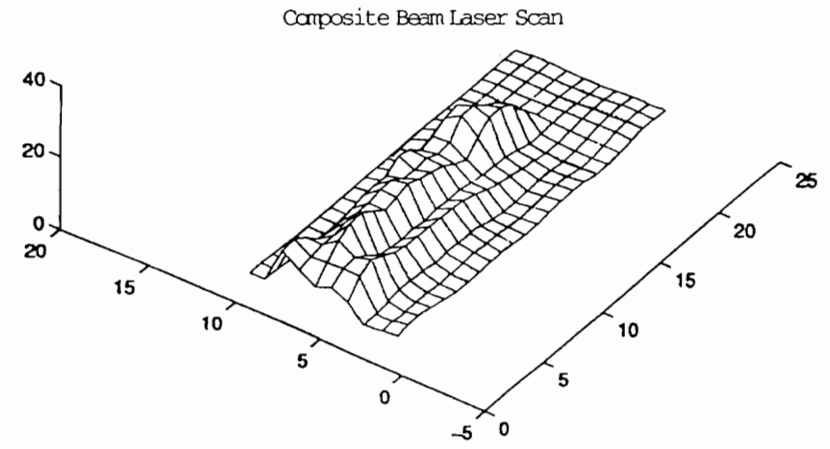

Figure 1.2 Quantitative damage detection methods, such as Ultrasonics, could be used only after a qualitative method has detected damage. The quantitative method provides the high resolution to assess the extent and the nature of the damage.

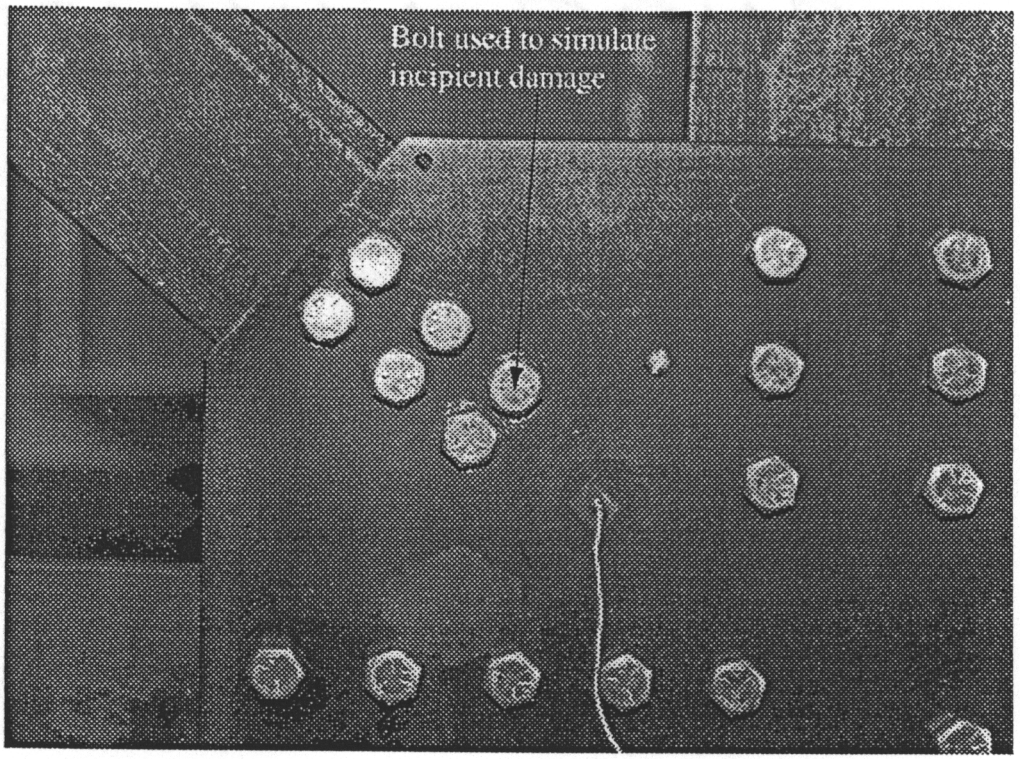

Figure 1.3 Incipient type of damage has no effect on the structural integrity or the strength of the part or structure being monitored. An example of incipient damage is a single bolt being loosened in a large joint.

Table 1.1 Qualitative and quantitative methods can be used in conjunction for an overall more efficient system for detecting and evaluating damage.

Qualitative vs. Quantitative Damage Detection		
	Pros.	**Cons.**
Qualitative Damage Detection Method	• Real time monitoring • Low cost of operation • No down time	• Low resolution
Quantitative Damage Detection Methods	• High resolution • Predicts size of damage • Predicts type of damage	• Down time • Bulky equipment • Needs direct access

1.2 OBJECTIVES

Based on the discussion made on real-time health monitoring made in the previous section, the objective of this research is to develop a qualitative real-time non-destructive evaluation technique. This method needs to be adaptable to most existing structures. It must operate in a non-intrusive manner and have the ability to detect very small structural damage. Based on these requirements, an impedance-based health monitoring technique which will be introduced in the next section, will be developed.

1.3 IMPEDANCE-BASED HEALTH MONITORING

The real-time health monitoring technique that will be presented in the thesis is impedance-based and relies on tracking the high frequency point impedance of a structure. The impedance-based health monitoring technique utilizes the change in the dynamic response (due to damage) to qualitatively identify damage. But, it is different from modal analysis-based methods. The fundamental difference lies in the frequency used to interrogate the structure, i.e., excite and sense the resulting vibration magnitude and phase. The frequencies used in this technique are much higher than those typically used in modal analysis-based methods. To sense incipient type damage, which dose not result in any measurable change in the structure's global stiffness properties, it is necessary for the wavelength of the excitation to be smaller than the characteristic length of the damage to be detected. Finding the damage when it is at an incipient level and before the global stiffness integrity is compromised, is most useful. This is because it can provide us with a warning before actual failure occurs.

The modal analysis-based techniques, since they typically rely on lower-order global modes, are not sensitive to incipient type damage. The damage, generally, must be of a global scale for it to cause an experimentally measurable change in the lower-order global

frequencies and modes. The other serious limitation of the modal analysis methods is the extreme sensitivity of the frequencies and modes to the boundary conditions. For example: aircraft structures, changes in the mass and the stiffness are part of the normal operation of the aircraft, e.g., consumption of fuel from the wing fuel cells, retraction and extension of landing gear, release of external stores, movement of control surfaces and flaps, etc. Simulation of all possible normal usage changes and their effect on the modal parameters is impossible to store as well as to distinguish them from damage. Even under very controlled conditions, it would be extremely difficult to reproduce the aircraft for modal testing in the same configuration in which the original data was acquired.

The impedance-based technique utilizes small piezoelectric (PZT) patches to provide high-frequency excitation, typically in the high kHz range, to the structure being monitored. By using the direct and the converse electromechanical properties of the PZT material, the simultaneous actuation and sensing of the structural response is possible. The variation in the electrical impedance of a PZT bonded to the structure of interest, while driven by a fixed alternating electric field over a frequency range, is analogous to frequency response but has a much higher resolution and is more easily obtained. The size of the PZT actuator/sensor is typically small (less than 0.5 sq. in., 0.01 in. thick), allowing for a non-intrusive installation. Electrical high-frequency excitation at low power is another benefit of the solid-state PZT actuator/sensor. High-frequency excitation provides two benefits: the response is dominated by local modes and incipient damage like small cracks, loose connections, and de-laminations, producing measurable changes in the impedance characteristics. The high frequencies also limit the actuation/sensing area. Thus it is possible to say with certainty that the change in impedance is due to damage in the sensing area and not due to a change in the far-field boundary conditions, such as mass loading, etc., which may be part of the normal usage of the structure. Localization is the unique feature which makes this impedance-based technique practical for implementation on real complex structures. Another very significant advantage of this

technique is that it relies on well-developed high frequency electrical impedance instrumentation. More elaborate details of the impedance-based technique will be presented in chapter 2.

1.4 APPLICATIONS

Qualitative impedance-based health monitoring can be adapted to almost any existing complex structure or incorporated into any new structure that would benefit from real time monitoring. A prime example is to use this technique on existing bridge structure. A bridge could benefit from a real-time monitoring system. Bridges require lots of unnecessary inspections that consume large amounts of time and money. These inspections are often very hard to complete and revel nothing. Fig. 4 is an example where qualitative health monitoring could have prevented a catastrophic failure.

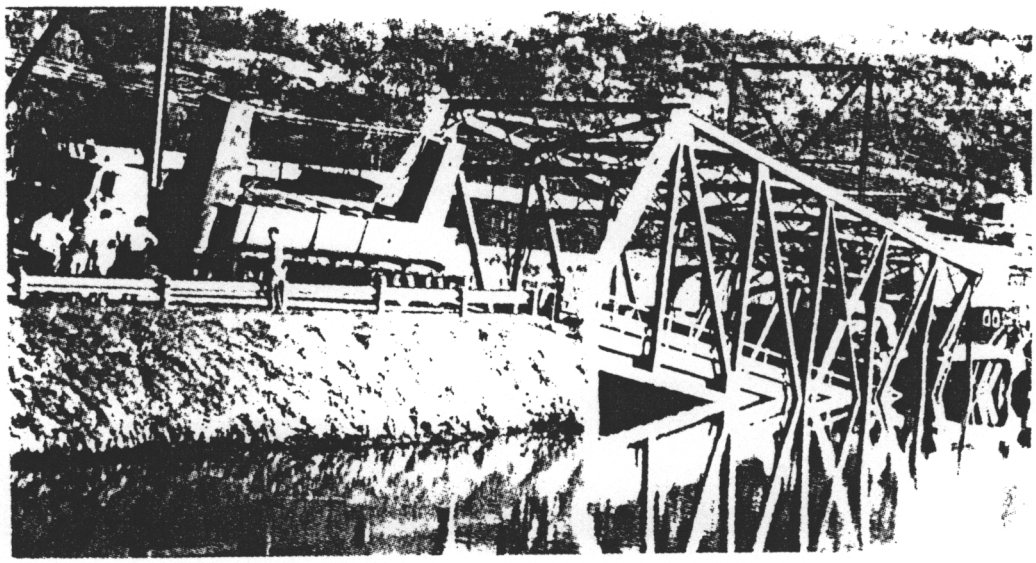

Figure 1.4 Because quantitative methods are not real time, the damage often becomes catastrophic before it is detected. The failure of this bridge started with incipient type damage at locations of high stress that could have been detected using qualitative methods.

Table 1.2 gives a brief list of some of the applications for this qualitative health monitoring technique. This list is in no way complete as there are a vast number of custom applications for this type of real-time monitoring.

Table 1.2 Qualitative damage detection can reduce the maintenance cost and the down time for many types of applications.

Applications of Qualitative Damage Detection:
Monitoring the bond in Composite patch repair of aircraft
Monitoring the bond in Composite patch repair of civil structures
Corrosion and erosion detection
Bridge integrity monitoring
Steel structural monitoring
Automotive applications such as suspension integrity monitoring
Space structural monitoring
Ship hull integrity monitoring

The application of this health monitoring technique is made easier because we often know where the high areas of stress will occur. Incipient type damage occurs at these areas of high stress and strain. High areas of stress are starting places for cracks, loose bolts, and bent or deformed members. The joints of a bridge are examples of critical areas that could be monitored for incipient type damage. By positioning the sensors at these areas we are able to detect the incipient damage before it causes failure.

1.5 THESIS ORGANIZATION

This thesis will present the impedance-based health monitoring technique. Included are an in-depth look at the mechanics of impedance-based health monitoring, a brief look at the electromechanical modeling that describe this technique; application involving case studies; results of the tests performed; and a discussion of issues that need further understanding.

CHAPTER 2

THEORY

In this chapter we will lay out the fundamental principles of the impedance-based health monitoring technique under study. We will also discuss the properties of the piezoelectric material used for its implementation; and show the details of the formulation that describe the modeling equations of this technique.

2.1 IMPEDANCE-BASED HEALTH MONITORING

Impedance-based health monitoring uses mechanical impedance to actively measure the integrity of material systems. This impedance is measured through the use of a piezoelectric (PZT) material. This PZT material acts as the actuator and the sensor for the system. The electrical impedance is coupled to the mechanical impedance so any structural change will show up as a change in the electrical impedance measurements.

2.1.1 MECHANICAL IMPEDANCE

Mechanical impedance is defined as the ratio of the applied force to the resulting velocity. Similarly, electrical impedance is the ratio of the applied voltage and the resulting current. Electromechanical transducer materials, such as piezoelectric material, provide a means to couple the mechanical and electrical impedance. This allows for the extraction of mechanical impedance information from a purely electrical impedance measurement.

$$Z(\omega) = \frac{F(\omega)}{\dot{x}(\omega)}, \tag{1}$$

$$Y = \frac{1}{Z(\omega)}, \tag{2}$$

where Z(ω) is the mechanical impedance, F(ω) is the input force, and $\dot{x}(\omega)$ is the resulting velocity. Y(ω) is the admittance, the reciprocal of the impedance.

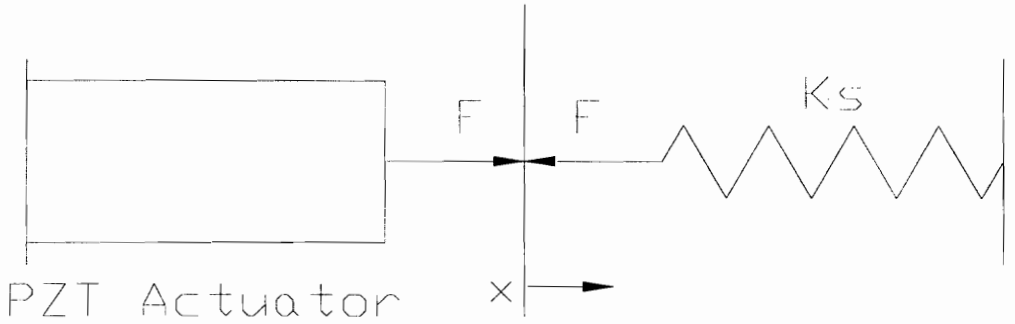

Figure 2.1 A spring driven by a PZT actuator.

The impedance of a structure is dependent of the frequency of excitation. This relationship can be seen in the simple example of the spring-mass-damper (SMD) system shown in Fig. 2.2

$$Z = c + m \cdot \frac{\omega^2 - \omega_n^2}{\omega} \cdot i, \tag{3}$$

where c is the damping coefficient, m the mass, ω the excitation frequency, ω_n the resonant frequency of the SMD system.

The resonant frequency is given by the following relationship:

$$\omega_n = \sqrt{\frac{K_s}{m}}, \tag{4}$$

where: K_s is the spring constant.

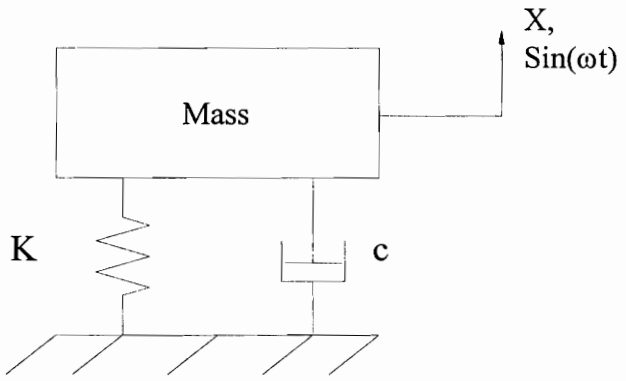

Figure 2.2 The mechanical impedance of a structure is dependent on the driving frequency, ω, of the system. This impedance changes with any change in the physical properties of the system.

The mechanical impedance of all SMD systems is dependent on the structural boundary conditions. Changing any of the properties of this system will result in a change of the impedance. An example of the impact of structural changes on the mechanical impedance is seen in Fig. 2.2. The solid line represents the systems impedance before any structural change. The dotted line represents a change in the mechanical impedance of the SMD corresponding to a small difference in the damping coefficient of the SMD.

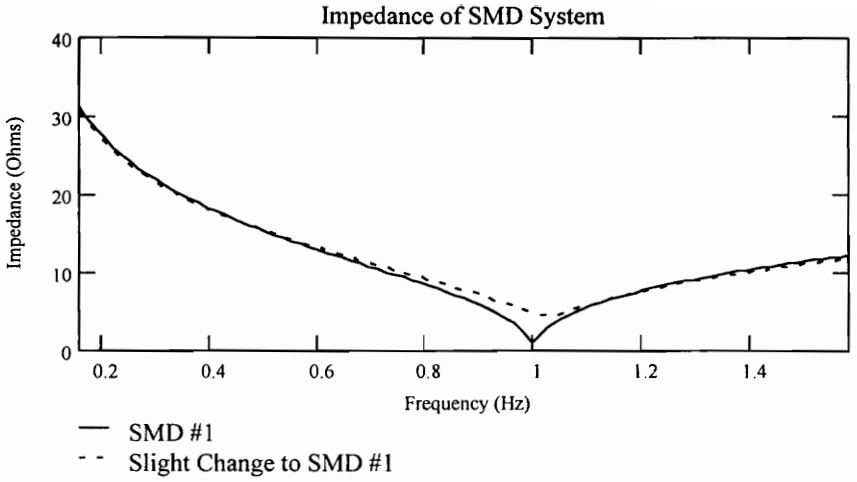

Figure 2.3 The mechanical impedance for the single-degree-of-freedom SMD system is graphically shown above. A change in the physical properties of the system resulted in a change in the impedance.

2.2 DYNAMIC ANALYSIS USING IMPEDANCE

The impedance method is used to analyze the dynamic characteristics of different structural systems. The interactions between a PZT actuator/sensor and structures are governed by the dynamic characteristics of the PZT actuator/sensor and the dynamic characteristics of the structure, i.e., the structural impedance. (Rogers, 1994)

In order to describe the electromechanical relations that describe impedance-based health monitoring we need to start at the beginning with the force-displacement relation that exists between the PZT actuator/sensor and the structure. This relation can be described as follows:

$$F = K_A \cdot (x - \Lambda), \tag{5}$$

where x is the displacement, F is the force exerted by the actuator, Λ is the free induced displacement of the PZT, and K_A is the static stiffness of the PZT given by:

$$K_A = \frac{\bar{Y}_{22}^E \cdot w_a \cdot h_a}{l_a}, \tag{7}$$

where w_a, h_a, and l_a are the width, thickness, and length of the PZT actuator/sensor, respectively, $\bar{Y}_{22}^E = Y_{22}^E(1 + i \cdot \varsigma)$,the complex modulus of the PZT at zero electric field, and ς is the mechanical loss factor of the PZT. Λ is the free-induced strain displacement of the actuator given by:

$$\Lambda = d_{32} \cdot E \cdot l_a, \tag{8}$$

where d_{32} is the piezoelectric constant and E is the electric field.

For a dynamic application, as in impedance-based health monitoring, the force-displacement relation needs to be modified using the relation of the force-displacement:

$$F = -Z \cdot \dot{x}, \tag{8}$$

Note: A negative sign is used because the SMD system is acting against the force F.

and mechanical impedance from Eq. 3. Assuming a harmonic motion ($\dot{x} = i \cdot \omega \cdot x$), the dynamic expression for the force is defined as:

$$F = -\left[c + m \cdot \frac{\omega^2 - \omega_n^2}{\omega} \cdot i\right] \cdot [i \cdot \omega \cdot x]. \tag{9}$$

Eq. 9 can be further simplified:

$$F = -\left[c \cdot i \cdot \omega - m \cdot (\omega^2 - \omega_n^2)\right] \cdot x = -K_D \cdot x\,, \tag{10}$$

where K_D is the dynamic stiffness.

The dynamic force-displacement relation can now be determined from Eq. 10 and Eq. 5 as:

$$F = -\frac{K_D \cdot K_A}{K_D + K_A} \cdot \Lambda\,. \tag{11}$$

The dynamic stiffness is frequency dependent (shown in detail by Liang et al., 1993a) hence, the force, F, exerted on a structure by the integrated actuator/sensor is also frequency dependent. In-depth details of the various approaches, including the static approach (Crawley and deLuis, 1990), dynamic finite element approach (Ha et al., 1992), and the impedance approach, can also be found in Liang et al. (1993a).

2.3 CHARACTERISTICS OF PIEZOELECTRIC MATERIAL

Piezoelectric material acts both as a sensor and an actuator to the host structure to which it is bonded to. There is a direct effect and a converse effect of the PZT material. When a PZT is subjected to a mechanical stress it generates an electric change (direct effect); conversely, when a PZT encounters an applied electric field it generated a mechanical

strain (converse effect). For a linearly acting piezoelectric material, the constitutive equations that describe the interaction between the electrical and mechanical variables are given by:

$$S_2 = \bar{s}_{22}^{E} \cdot T_2 + d_{32} \cdot E, \tag{12}$$

$$D_3 = \bar{\varepsilon}_{33}^{T} \cdot E + d_{32} \cdot T_2. \tag{13}$$

The mechanical variables in the above equations are S_2, the mechanical strain and T_2, the mechanical stress. The electrical variables are E, the electric field and D_3, the electric displacement. Other variables include: $\bar{s}_{22}^{E}$, the complex compliance at zero electric field, $d_{32,}$ the piezoelectric constant, and $\bar{\varepsilon}_{33}^{T}$, as the complex dielectric constant at zero stress.

Many applications that use the PZT material take advantage of only part of the materials capabilities. However, this qualitative damage detection method uses both the converse and the direct effect of the material. The piezoelectric material is bonded to the structure and driven by a fixed alternating field. This alternating field induces vibrations in the structure. At the same time the vibrational response, which is characteristic of the particular structure, modulates the current flow in the PZT. This modulation represents the degree of mechanical interaction between the PZT and the structure over different frequencies. This impedance pattern serves the same purpose as the traditional transfer function.

2.4 COUPLED ELECTRO-MECHANICAL MODELING

The electromechanical modeling that qualitatively describes the acquisition of the coupled electrical and mechanical impedance is described below. The PZT is considered a thin bar undergoing axial vibration in response to an applied alternating voltage. The dynamic interaction of the PZT and the structure can be seen in Fig. 2.3.

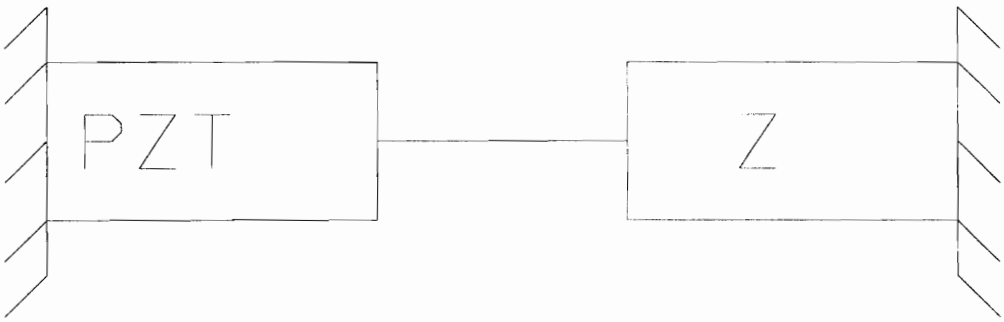

Figure 2.4 A schematic illustration of a PZT lumped parameter system. The PZT serves as an actuator for the one-degree-of-freedom spring mass damper system which is representative of the structural impedance (Z).

The PZT is considered fixed at one end, while the other end is attached to an external structure. The dynamic interaction is determined by the coupling one of the constitutive equations, the converse effect, with both the PZT and the structure's equilibrium, compatibility, and equations of motion. The first assumption made about this process is that the PZT only expands in the Y direction from the applied electric field in the Z direction. The equation of motion for a PZT vibrating in the Y direction is described:

$$\rho \cdot \frac{\partial^2 V}{\partial t^2} = \bar{Y}_{22}^{E} \frac{\partial^2 V}{\partial y^2}, \tag{14}$$

where V is the displacement in the Y-direction, ρ is the density of the PZT. Solving Eq. 14 by separating the displacement V into time and spatial domain solutions.

$$V = \bar{V} \cdot e^{i \cdot \omega \cdot t} = (A \cdot \sin(k \cdot y) + B \cdot \cos(k \cdot y)) \cdot e^{i \cdot \omega \cdot t}, \tag{15}$$

Where

$$k^2 = \omega^2 \cdot \frac{\rho}{\bar{Y}_{22}^E}. \tag{16}$$

Note: a bar over a variable indicates its spatial component, except in the case of complex material properties, such as $\bar{\varepsilon}_{33}^T$ and $\bar{s}_{22}^E$.

The equation of motion, as given by Eq. 14, requires two boundary conditions to yield a solution. This information will be found in the equilibrium and compatibility relations between the structure and the PZT. The PZT is connected to a structure which is represented by its impedance Z (Fig. 2.3). A simple expression for this impedance is given by Eq. 4 for a single degree of freedom SMD system. The equilibrium and compatibility relation between the PZT and the structure can be described by:

$$T_{2_{y=l_a}} = \bar{T}_{2_{y=l_a}} \cdot e^{i \cdot \omega \cdot t} = -\frac{Z \cdot \bar{V}_{y=l_a} \cdot i \cdot \omega}{w_a \cdot h_a} \cdot e^{i \cdot \omega \cdot t}. \tag{17}$$

The displacement V, as given by Eq. 15, requires two boundary conditions. Equation 17 provides one of these conditions. The other is given at y = 0 by: $V_{y=0} = 0$. This leads to B = 0.

Using the converse constitutive relation we can solve for the resulting strain from the equilibrium and compatibility relations. Substituting Eq. 17 into Eq. 12 yields the following:

$$\bar{S}_2 = \frac{d\bar{V}}{dy}\Big|_{y=l_a} = -\bar{s}_{22}^{E} \cdot \frac{Z \cdot \bar{V}_{y=l_a} \cdot i \cdot \omega}{w_a \cdot h_a} + d_{32} \cdot \bar{E}. \tag{18}$$

The coefficient, A, in Eq. 15, can now be solved using Eq. 18.

$$A = \frac{d_{32} \cdot \bar{E}}{k \cdot \cos(k \cdot l_a) + \frac{\bar{s}_{22}^{E} \cdot Z \cdot i \cdot \omega}{w_a \cdot h_a} \cdot \sin(k \cdot l_a)}. \tag{19}$$

The mechanical impedance of a structure is introduced here to further simplify the derivation.

The actuator response can be described as the ratio of the excitation force to the velocity response, that is:

$$Z_a = -\frac{K_a(1+\eta \cdot i)}{\omega} \cdot \frac{k \cdot l_a}{\tan(k \cdot l_a)} \cdot i. \tag{20}$$

The mechanical impedance of the PZT actuator is based on the assumption that the PZT behaves like a passive material and has no electric coupling.

This expression for the mechanical impedance can be used to further simplify the expression for the coefficient, A as:

$$A = \frac{Z_a \cdot d_{32} \cdot \bar{E}}{k \cdot \cos(k \cdot l_a) \cdot (Z_a + Z)}. \tag{21}$$

The output displacement of the PZT actuator can be solved for as follows:

$$\bar{x} = \bar{V}_{y=l_a} = \left[\frac{Z_a \cdot d_{32} \cdot \bar{E}}{k \cdot \cos(k \cdot l_a) \cdot (Z_a + Z)} \right] \cdot \sin(k \cdot l_a), \tag{22}$$

remembering that $\bar{V}$ is the spatial component of the output displacement of the PZT.

Equation 22 is further simplified yielding the output displacement field:

$$\bar{x} = \bar{V}_{y=l_a} = \frac{Z_a \cdot d_{32} \cdot \bar{E} \cdot l_a}{Z_a + Z} \cdot \frac{\tan(k \cdot l_a)}{k \cdot l_a}. \tag{23}$$

The strain field can be calculated from Eq. 15 and Eq. 18 as follows:

$$\bar{S}_2 = \frac{d\bar{V}}{dy}\Big|_{y=l_a} = \frac{Z_a \cdot d_{32} \cdot \bar{E}}{Z_a + Z} \cdot \frac{\cos(k \cdot y)}{\cos(k \cdot l_a)}. \tag{24}$$

The stress field can be solved for by using Eq. 24 and Eq. 12 as follows:

$$\bar{T}_2 = \frac{\bar{S}_2 - d_{32} \cdot \bar{E}}{\bar{s}_{22}^E}, \tag{25}$$

substituting $\bar{S}_2$, the strain field, and simplifying further:

$$\overline{T}_2 = \frac{\left[\frac{Z_a \cdot d_{32} \cdot \overline{E}}{Z_a + Z} \cdot \frac{\cos(k \cdot y)}{\cos(k \cdot l_a)}\right] - d_{32} \cdot \overline{E}}{\overline{s}_{22}^E}, \tag{26}$$

and furthered simplified to the expression for the stress field:

$$\overline{T}_2 = \left[\frac{Z_a}{Z_a + Z} \cdot \frac{\cos(k \cdot y)}{\cos(k \cdot l_a)} - 1\right] \cdot d_{32} \cdot \overline{Y}_{22}^E \cdot \overline{E}. \tag{27}$$

The electric displacement field can now be solved for using Eq. 27 and Eq. 12 as follows:

$$\overline{D}_3 = \overline{\varepsilon}_{33}^T \cdot \overline{E} + d_{32} \cdot \overline{T}_2, \tag{28}$$

which, after substitution of $\overline{T}_2$, the stress field, simplifies to:

$$\overline{D}_3 = \frac{Z_a \cdot d_{32}^2 \cdot \overline{Y}_{22}^E \cdot \overline{E}}{Z_a + Z} \cdot \frac{\cos(k \cdot y)}{\cos(k \cdot l_a)} + (\overline{\varepsilon}_{33}^T - d_{32}^2 \cdot \overline{Y}_{22}^E) \cdot \overline{E}. \tag{29}$$

The electric current is found using

$$I = i \cdot \omega \iint D_3 dx dy, \tag{30}$$

which yields, after substitution of Eq. 29:

$$I = \bar{I} \cdot e^{i\cdot\omega\cdot t}, \tag{31}$$

where

$$\bar{I} = i \cdot \omega \cdot \bar{E} \cdot w_A \cdot l_A \cdot \left(\frac{d_{32}^2 \cdot \bar{Y}_{22}^E \cdot Z_a}{Z + Z_a} \cdot \frac{\tan(k \cdot l_A)}{k \cdot l_A} + \bar{\varepsilon}_{33}^T - d_{32}^2 \cdot \bar{Y}_{22}^E \right). \tag{32}$$

Noting that the electric field is: E=V/h_A, the electrical admittance, Y=I/V, can be expressed from Eq. 25 as follows:

$$Y = i \cdot \omega \frac{w_a \cdot l_a}{h_a} \cdot \left(\frac{d_{32}^2 \cdot \bar{Y}_{22}^E \cdot Z_a}{Z_a + Z} \cdot \frac{\tan(k \cdot l_A)}{k \cdot l_A} + \bar{\varepsilon}_{33}^T - d_{32}^2 \cdot \bar{Y}_{22}^E \right) \tag{33}$$

The expression $\tan(kl_a)/kl_a$ is close to one for the frequency range used in most Impedance-based NDE techniques (generally above 10 kHz). Therefore, the expression for the coupled electro-mechanical admittance reduces to:

$$Y = i \cdot \omega \frac{w_a \cdot l_a}{h_a} \cdot \left(\bar{\varepsilon}_{33}^T - \frac{Z}{Z_a + Z} \cdot d_{32}^2 \cdot \bar{Y}_{22}^E \right) \tag{34}$$

The expression for the coupled electro-mechanical impedance, in the form of admittance, is shown above. The first term in Eq. (34) is the capacitive admittance of the free PZT, and this part shows up in the admittance pattern as the base-line gradual change in admittance with frequency. The second term includes the PZT's own mechanical impedance as well as the external structure's mechanical impedance. For a PZT bonded to a structure, its own impedance Z_a is fixed; therefore, it is the structure's impedance, Z which varies the contribution of the second term to the overall admittance. The contribution of the second term shows up in the admittance vs. frequency plots as sharp

peaks above the base line electrical capacitive admittance. Because these peaks correspond to specific structural resonance's, they constitute a unique pattern of the structures dynamic behavior. Therefore, "any" change in the impedance pattern is considered to be damage to the structure. This expression models the interaction of the PZT and the structure for dynamic analysis of material systems.

2.5 COUPLED ELECTRO-MECHANICAL IMPEDANCE

Although the mechanical impedance of a structure can be measured through the use of shakers, force gages, and accelerometers, it is the electrical impedance of the structure that is measured in this qualitative health monitoring technique. It is much easier to measure the electrical impedance than the mechanical impedance. This electrical impedance is functionally equivalent to a mechanical driving point impedance. The coupled electromechanical impedance is measured through a commercially available multipurpose impedance analyzer shown in Fig. 2.4. The acquisition can be described as follows: The impedance analyzer provides a constant voltage to the PZT transducer over a pre-set frequency range. The magnitude and phase of the steady state current draw (after transient decay) of the PZT is measured and the real and imaginary admittance (admittance is the reciprocal of impedance) is calculated. This process is repeated, each time incrementing the frequency, until the upper frequency limit is reached. This is known as the impedance or admittance pattern. The PZT material uses the applied voltage as the actuator, and the current measurement as the sensor. The current draw is the measurement of the structural interaction between the PZT actuator/sensor and the structure (Eq. 32).

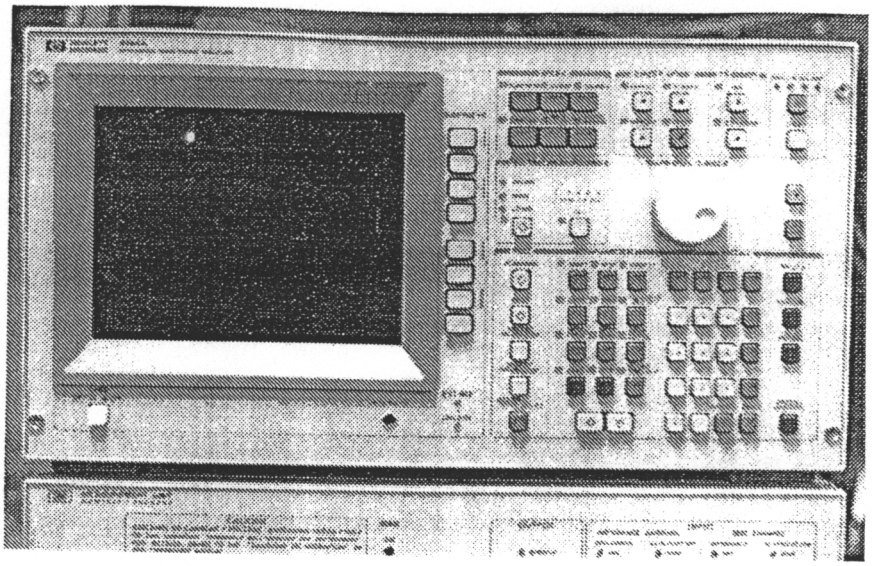

Figure 2.5 HP 4194A Impedance analyzer used to measure the electrical admittance of a structure.

The impedance pattern consist of a variation in the electrical impedance, which is analogous to the dynamic frequency response of the structure. This variation in the electrical admittance is due to two factors: 1) the electrically capacitive nature of the PZT and; 2) the interaction between the PZT and the structure to which it is bonded. The variation in the capacitive nature shows up as a gradual change in the impedance curve, whereas the structural interaction corresponds to sharp peaks that represent points of structural resonance, since the host structure represents a frequency dependent boundary stiffness. As stated in the introduction, the presents of damage in the structure being monitored will change the structural impedance, which will change the current draw by the PZT, which has the final effect of changing the electrical impedance. By monitoring changes in the electrical impedance measurements before and after damage, damage can thus be detected.

CHAPTER 3

EXPERIMENTAL RESULTS

In this chapter the impedance-based NDE technique will be applied to five case studies. The structures used in the case studies represent a wide variety of sizes, stiffness, masses, and applications. The premises in using such a wide array of structures is to demonstrate that the impedance-based technique can be successfully applied to many types of structures. Also, in each case studie, the focus will be given to a different aspect of the NDE technique, such as investigating the type of damage that can be detected, investigating the localized sensing area, and implementation on a wide network of sensors.

3.1 DAMAGE METRIC DEFINITION

Impedance-based health monitoring is tested on several different structures. In each test a small piece of piezoelectric material is bonded to the test structure at a "critical" area. Because this method is qualitative, the detailed analysis of the impedance or admittance graphs is not necessary to the success of this technique. A single number for each test is obtained to simplify the interpretation of the admittance changes. The damage metric used for this comparison is defined as:

$$M = \sum_{i=1}^{401} \left[\mathrm{Re}(Y_{i,1}) - \mathrm{Re}(Y_{i,2}) \right]^2 \tag{28}$$

where M represents the sum of the real admittance change squared. Other variables include: $Y_{i,1}$, the admittance of the PZT before the structure has been altered at frequency interval *i*; and $Y_{i,2}$, the admittance of the structure after the alterations at frequency interval *i*. The integer 401 represents the number of frequency steps used in each test. This damage metric is then normalized by choosing an arbitrary amount of damage, and assigning this damage a value of 100%; all other measurement are then compared to this known amount.

3.2 COMPOSITE PATCH REPAIR

Composite patch repair involves bonding a composite material to an arbitrary host structure in-order to repair a crack, corrosion, or some other structural flaw. This patch takes the place of replacing the entire damaged section. It is often impractical to replace the entire side of an aluminum structure when there is only a small damage. A composite patch prevents the damage (crack or tear) from spreading throughout the surface, thus eliminating the need to replace the entire panel. Normally after a crack or tear appears in a panel, the entire section must be replaced. Often the size of the crack is many times smaller than the panel, meaning a large repair for a small crack. Composite patch repair is becoming an important concept for the maintenance of certain structures. Composite patch repair has several advantages over conventional repair; 1) lower cost for repairs, 2) shorter structural down time, 3) better structural integrity (Chung, 1991). It is clear that composite patch repair is a growing technology; however, the success of all forms of composite patch repair is dependent on the integrity of the bond between the host structure and the high strength composite patch. If this bond fails then the damage can cotinue to spread. Impedance-based damage detection provides a real-time method for monitoring the integrity of this bond over the service life of the structure as well as the

monitoring of the crack growth. This will facilitate the application of the composite patch repair, and lower the maintenance costs associated with the repair.

Impedance-based health monitoring is tested using an aluminum plate and a de-bonded composite patch. The objective is to qualitatively detect the de-bond between the plate and the composite patch and to detect a growth in the repaired crack(Chaudhry et al., 1995). Presented in this thesis is a summary of the tests and results. Three plate specimens were fabricated for this experiment and are considered representative of actual composite repair. A typical specimen consists of a 200 x 70 mm, 12-ply composite patch bonded to a 250 x 200 mm, aluminum plate (see Fig. 3.1). The goal is to find the occurrence of a de-bond between the base aluminum plate and the composite patch.

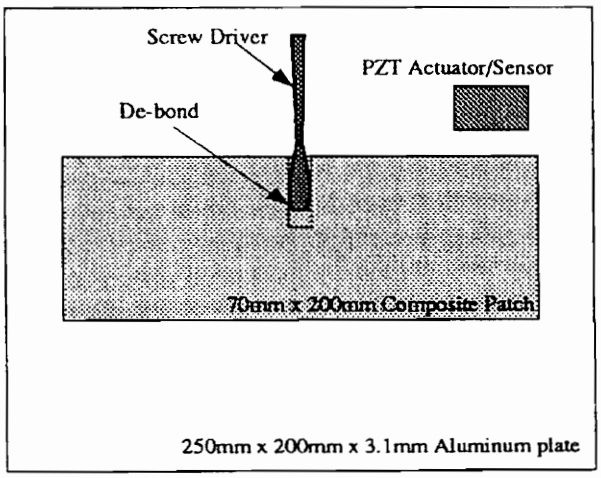

Figure 3.1 Geometry of the plate test specimen received from E-Systems used to monitor the bond quality between the composite patch and the aluminum plate.

The PZT actuator/sensor is wired to the HP-4194A impedance analyzer for the acquisition of the impedance measurements. The test is conducted with the plate hanging from one point. The data is transferred to a PC computer for analysis. The frequency ranges used in the experiments are shown in Table 3.1 below.

Table 3.1 Frequency ranges used for the acquisition of the impedance measurements.

Large Frequency Interval (kHz)	1-10	10-20		20-30	30-40
Smaller Frequency Interval (kHz)	2.1-3.7	14.5-15.5	18.0-19.0	22.5-26.0	34.2-35.8

Many different frequency ranges are tested to find the optimum range that exhibits the most interaction between the PZT and the host aluminum plate. A good interaction in the admittance measurements shown as large peaks and valleys above and below the gradual base line capacitive nature of the PZT. For this test, the frequency range with the most interaction is 10-20 kHz. Smaller frequency ranges are then chosen to obtain higher resolution in areas that exhibit large activity. The maximum number of data points for any interval is 400; therefore, when the range is narrowed, the resolution goes up.

The de-bond is created by inserting a flattened screwdriver between the composite patch and the base-plate (see Fig. 3.1). Three types of damage are simulated corresponding to three screw-driver insertion depths, ¼, ½, and ¾ in. deep respectively between the composite and the base-plate. This simulated damage represents incipient damage to the bond. Although the patch would continue to function if this damage went un-detected, a failure would almost be certain due to the weakening bond layer.

The impedance measurements are shown for visual comparison and verification of the impedance method. The impedance magnitude plots corresponding to de-bonds of ¼, ½, and ¾ in. are shown in Fig. 3.2 and 3.3 for a larger frequency and smaller frequency interval, respectively. The changes in the impedance measurements over the large frequency interval are difficult to see (10 - 20 kHz, Fig. 3.2). However, the de-bond

produces a clear shift in the impedance measurements in the smaller frequency interval (18 - 19 kHz, Fig. 3.3).

Because this method is qualitative, the detailed analysis of modal peaks or frequency shifts in the impedance graphs (Fig. 3.2 and 3.3) is not necessary to the success of this technique. A single number for each test is obtained to simplify the interpretation of the changes using the damage metric in Eq. (28). The normalization of this de-bond data produces a damage comparison chart seen in Fig. 3.7. In this normalization, the ½ in. de-bond is considered the 100% damage, and all other values are normalized to this value and compared. A damage index larger than 100% indicates damage that is larger than the reference damage. This process can further be simplified by the use of a computer to compare many different locations and report the results only when a threshold value is reached.

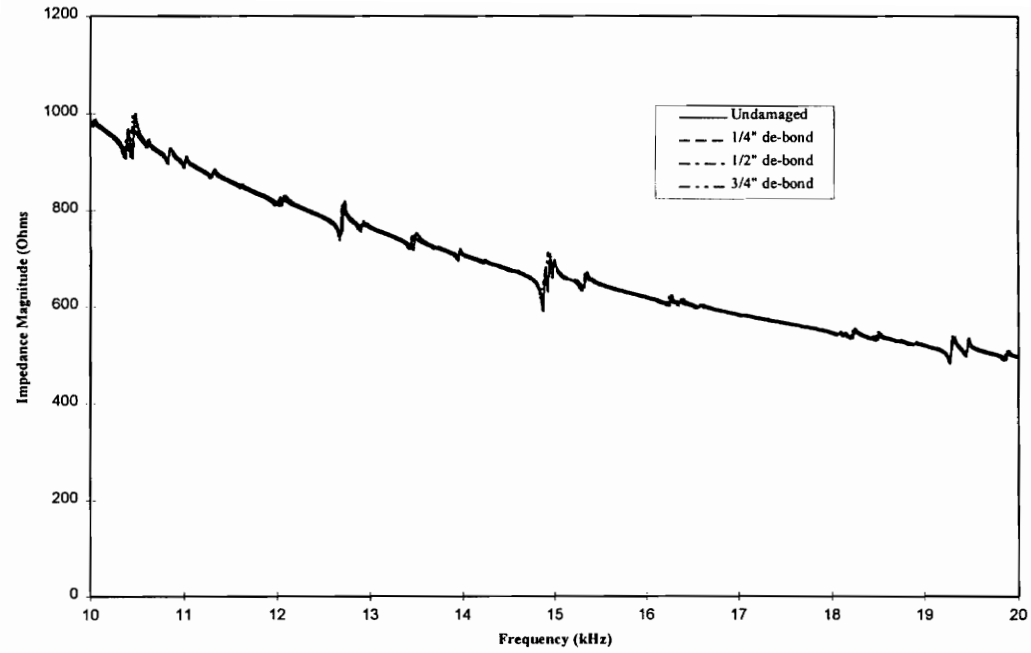

Figure 3.2 The effect of de-bonding on impedance magnitude is not clear over a large frequency interval.

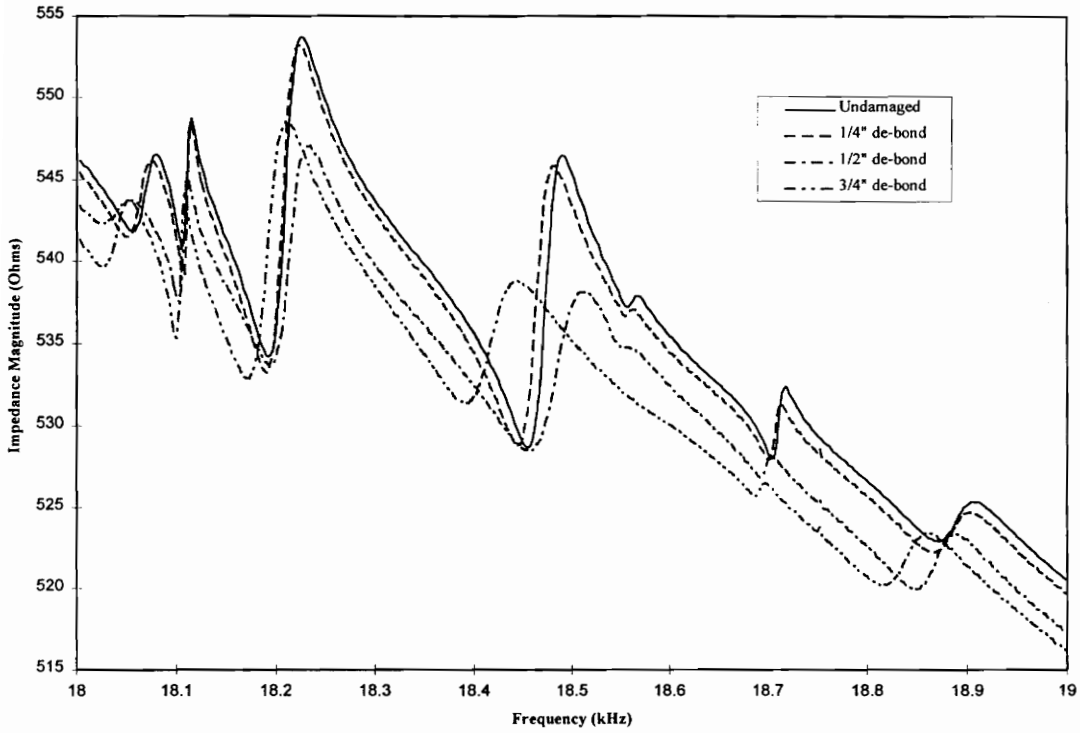

Figure 3.3 The effect of de-bonding is clear over the shorter frequency interval.

A specially prepared dog-bone specimen is used to monitor the crack growth under a composite repair patch using impedance-based health monitoring. The test specimen can be seen in Fig. 3.4. The specimen contains a damaged section that is covered by a composite patch. There were two types of composite patches used: Graphite/Epoxy and Boron/Epoxy. Each specimen was subjected to a cyclic load causing a crack growth. The admittance measurements before and after the cyclic loading are compared. This comparison can be seen in Fig. 3.5 and 3.6 respectively.

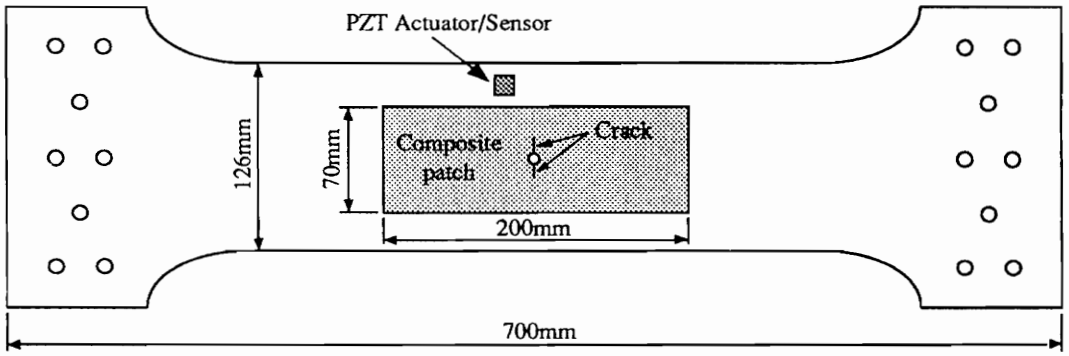

Figure 3.4 Geometry of dog-bone specimen used to monitor the crack growth under a composite repair patch

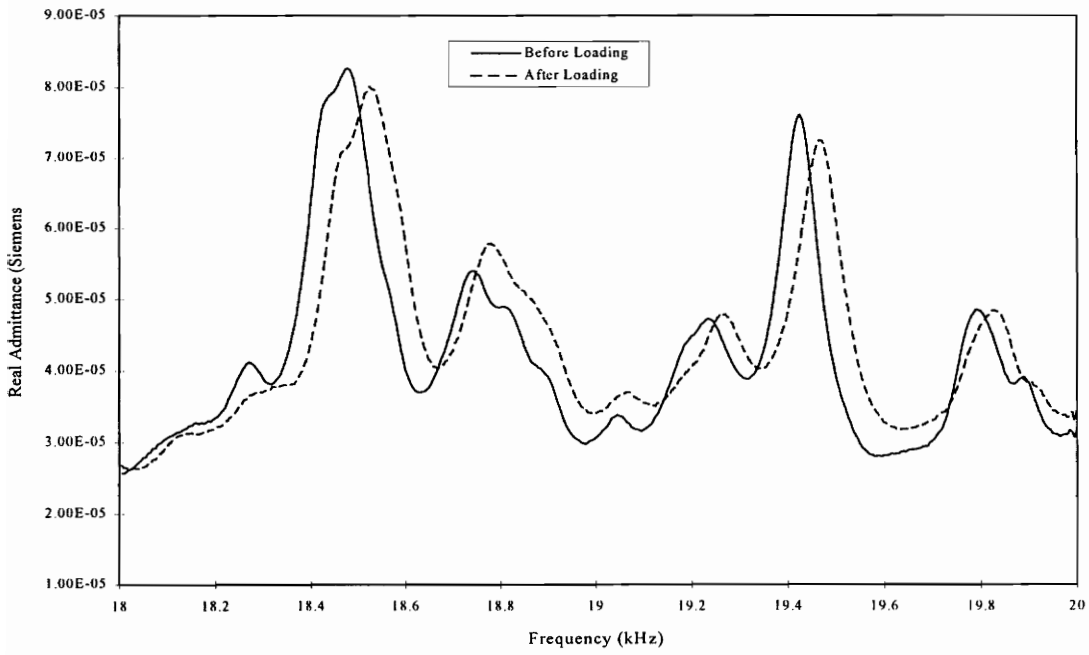

Figure 3.5 Effect of crack growth on the admittance measurements of the dog-bone specimen with graphite/epoxy patch.

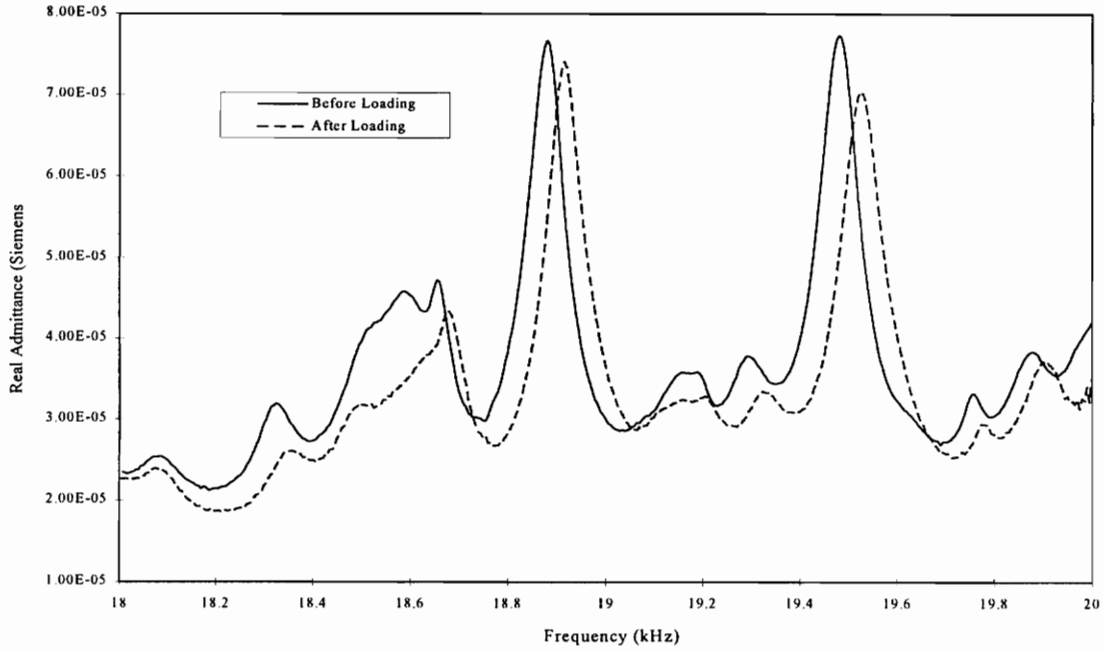

Figure 3.6 Effect of crack growth on the admittance measurements of the dog-bone specimen with boron/epoxy patch.

The change in the admittance measurements for the dog-bone specimen before and after crack growth is observed. Similar results were performed on a plain dog-bone specimen with the same results.

The normalized data, using the damage metric defined in Eq. (28), for the three levels of de-bond is presented in Fig. 3.7. The frequency range of 10-20 kHz was used for this comparison. Although the presents of damage was unclear in the large frequency interval

impedance plot (Fig. 3.2), the graph seen in Fig. 3.7 indicates how sensitive the technique is to the smallest de-bond. Three distinct levels of de-bond are seen in the qualitative comparison.

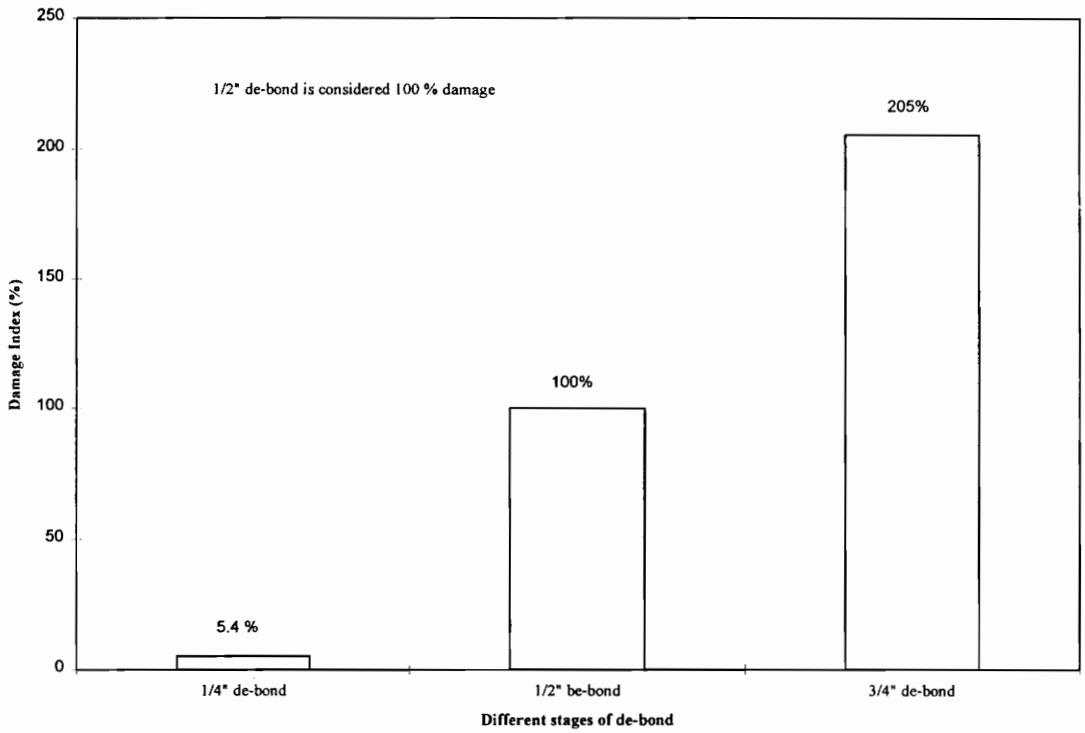

Figure 3.7 The different stages of de-bonding become clear when the data is presented in a qualitative manner.

Impedance-based health monitoring, for the detection of de-bonds and the monitoring of crack growth, has been shown to be a successful NDE method in composite patch repair applications. The high frequency excitation, coupled with the available impedance analyzer provides a great deal of sensitivity for detecting very minor de-bonds.

3.3 COMPLEX PRECISION PARTS

Qualitative health monitoring can be used as a real-time method for monitoring the integrity of complex parts. Currently there is a number of NDE techniques that are capable of detecting small cracks and incipient damage in small and complex parts. However, the current health monitoring techniques require that the mechanical system be taken out of service and disassembled in-order to find the damage. Impedance-based health monitoring will provide a health monitoring technique that can reduce a systems down time, and lower the maintenance cost of the system. This technique will be ideal for areas which, over the service life of the structure, have been identified as weak, and as yet are difficult to inspect.

Impedance-based health monitoring was tested on small precision gears. The objective is to qualitatively detect incipient damage in isolated areas, such as gear teeth (Lalande et al., 1996). Presented in this thesis is a detailed summary of the tests and results performed on the complex precision parts.

The impedance-based technique is tested on precision gears. Six 303 stainless steel precision gears are used for testing. Two of the six gears, referred to as type 1 gears, have 36 teeth, 2.25 inch nominal diameter, and a 0.375 inch thickness. The remaining four gears (Type 2) have 40 teeth, a 2.5 inch nominal diameter, and are 0.375 inches in thickness. All of the gears have a 16 pitch and are AGMA 10 quality. The gears used can be seen in Fig. 3.8. The piezoelectric actuator/sensor was bonded to the gear between the root diameter of the gear and the bore. The sizes of the PZT actuator/sensors used are 0.625 by 0.75 inches for type 1 gears and 0.625 by 1.0 inches for type 2 gears with a thickness of 0.01 inches. The size of the PZT allows for a non-intrusive bond to the gear. The initial tests indicated the optimum frequency range between 100 kHz and 275 kHz. This range exhibited the most dynamic activity (peaks and valleys).

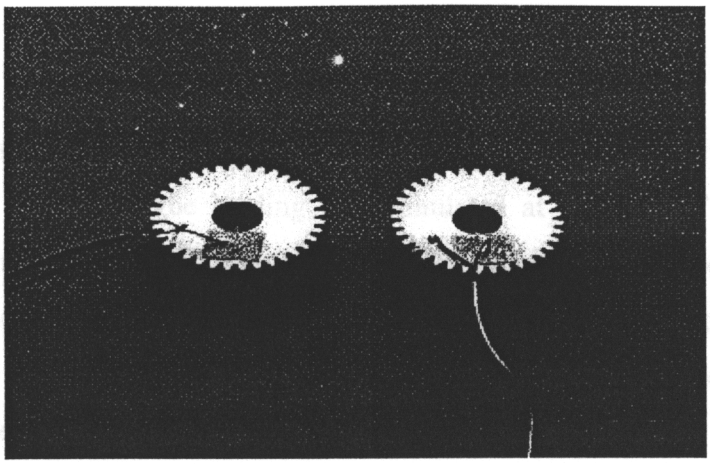

Figure 3.8 Precision gears with bonded PZT actuator/sensors that are used in the experimental testing.

The types of damage simulated on the precision gears is based on the most common types of damage seen by gears under normal operating conditions. There are two common failures of precision gears. These include abrasive wear from normal use and cracking due to bending fatigue. These types of damage are simulated as close as possible to best simulate real world situations. The type 2 gears were selected for the abrasive wear tests. The goal was to simulate the progressive stages of wear (seen if Fig. 3.9) on a tooth adjacent to the PZT actuator/sensor. The different levels of wear are simulated by filing the base of a tooth, using a standard steel file, that is adjacent to the PZT actuator/sensor. The impedance measurements are taken between each level of wear.

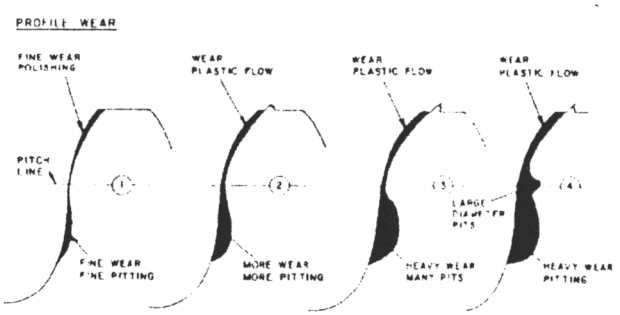

Figure 3.9 Progressive stages of wear in gears (Alban, 1985).

The damage resulting from bending fatigue was simulated on the type 2 gears. The crack resulting from such a fatigue loading was simulated at the root of a tooth using an electron discharge machine (EDM) with a 0.5 mm tungsten-brass electrode. In the first gear, an adjacent crack 0.18 inches deep is located at the base of a tooth above the PZT patch, while in the second gear, a distant crack 0.05 inches deep is located 90° from the PZT actuator/sensor (Fig. 3.10). This was done to verify the ability to detect damage anywhere in the gear.

Because the impedance-based technique is sensitive to incipient changes in the structure it can also be used as a quality assurance technique. High quality gears have corresponding natural frequencies. A shift in a gear's resonance represents a deviation in quality.

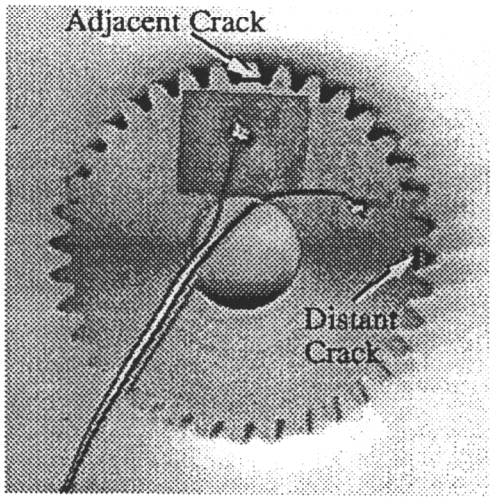

Figure 3.10 Locations of the tooth bending cracks on the experimental type 1 gears (one crack per one type 1 gear).

A quality assurance test is performed over a wide frequency range. The lower frequency ban of 1 kHz to 50 kHz is seen in Fig. 3.11 for the four type 2 gears used in the experiment. The vertical shift in the impedance measurements of the four gears is due to the PZT actuator/sensor. A vertical impedance shift is caused by small variations in the bonding layer, size, and the location of the PZT actuator/sensor witch differs from gear to gear. Thus, only the change in the peaks and valleys represent a difference in quality because this variation is due to the interaction between the PZT actuator/sensor and the structure (in this case a gear). Once the PZT is bonded to a structure a vertical shift can only be caused by new damage in the structure or by a change in the capacitive properties of the PZT actuator/sensor due to temperature variations (Krishnamurthy et al., 1996). The quality comparison (Fig. 3.11) reveals small variances in the resonance's at higher frequencies, but overall the changes were small enough to indicate good quality.

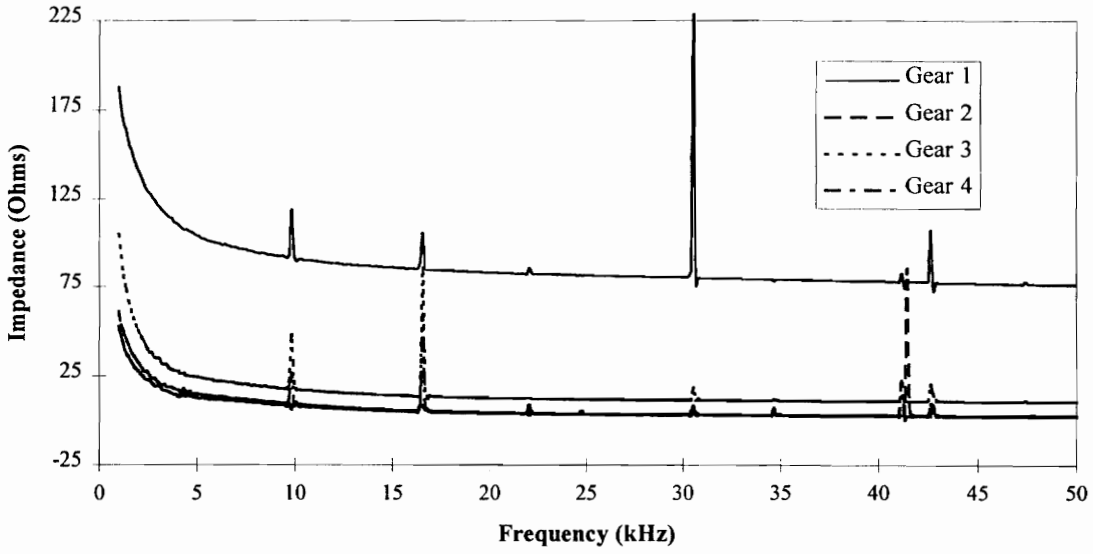

Figure 3.11 The impedance-based NDE technique can be used for quality control of precision parts. A deviation in the natural frequencies of the gear indicates a rejection. In this case, no gears were rejected.

The first damage that is simulated is abrasive wear. The impedance measurements for this damage are shown in Fig 3.12 for the 190 kHz - 200 kHz frequency range. The first level of abrasive wear was not detected, and is not shown in the figure. The second level of wear results in small differences in the impedance measurements. The differences become even grater at the third level of abrasive wear. The small amount of wear was created on a single tooth of the gear. The actual impedance changes may be even greater because abrasive wear usually occurs on many teeth throughout a gears life.

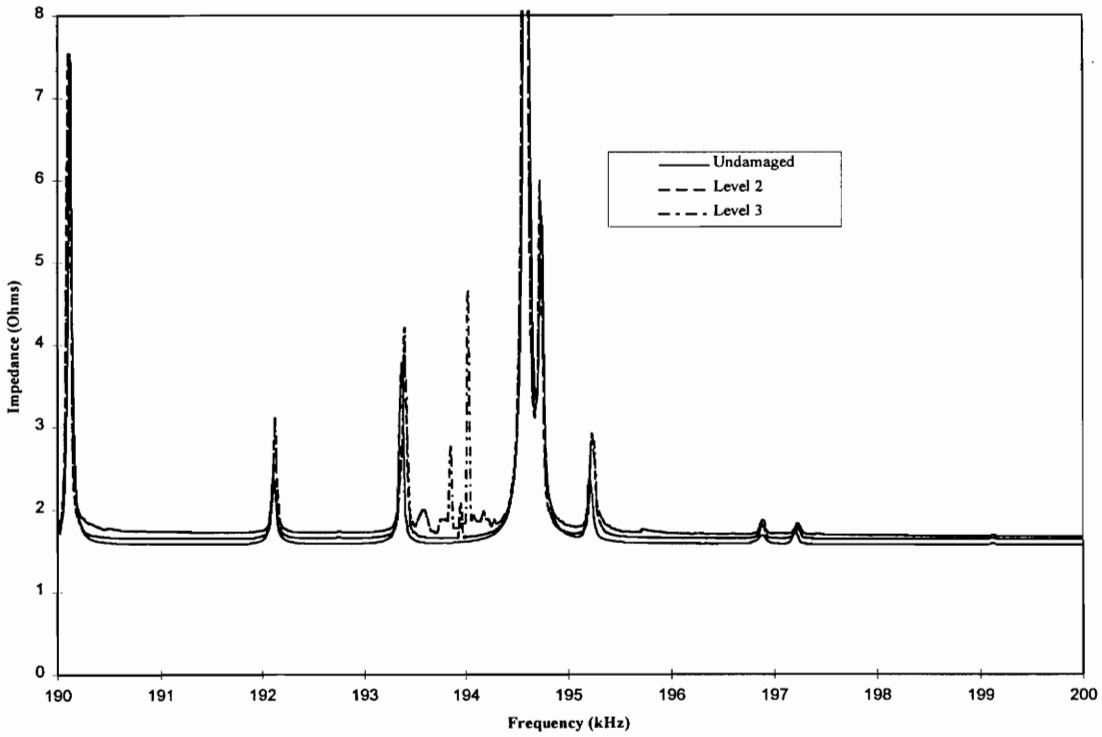

Figure 3.12 The effect of abrasive wear can be detected using the impedance-based NDE method.

The second type of damage simulated on the precision gears is fatigue bending cracks. Two separate tests are performed: the adjacent crack over a frequency interval of 175 kHz - 185 kHz and the distant crack over a frequency interval of 195 kHz - 205 kHz. The figures corresponding to the adjacent and distant crack tests are seen in Fig. 3.13 and 3.14 respectively. Both of these tests display a distinct change in the impedance measurements. The change is more significant in the adjacent crack test. This is due both to the adjacent crack being deeper, and the localization effect of the impedance-based technique. Nevertheless, any cracks in the gear can still be easily detected; a crack closer to the PZT actuator/sensor would only result in a larger damage index.

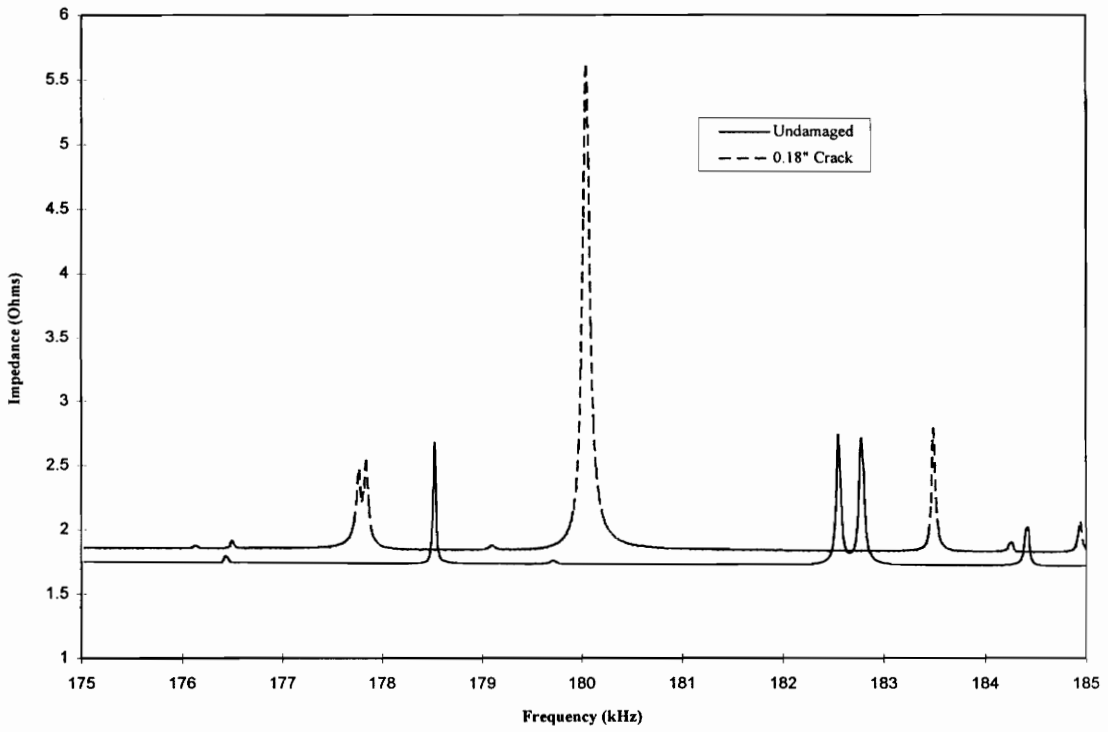

Figure 3.13 The change in the impedance measurements caused by a 0.18 in. deep crack of the tooth adjacent to the PZT actuator/sensor is significant.

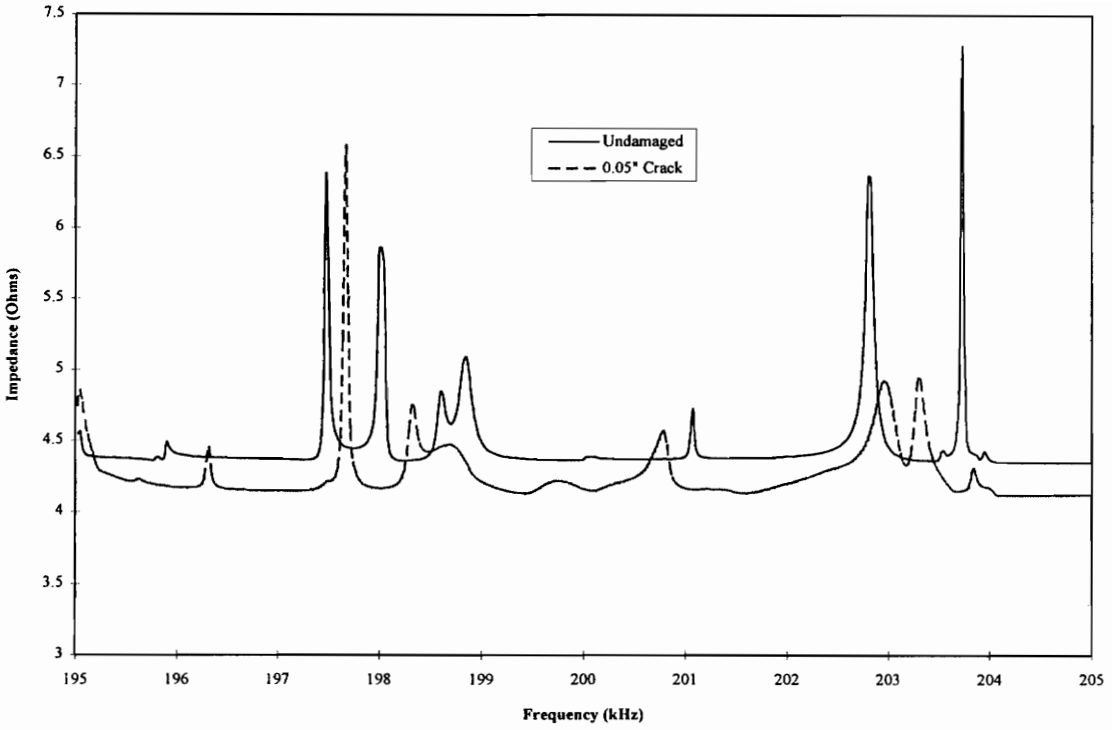

Figure 3.14 The change in the impedance caused by a 0.05 in. deep crack at the root of the tooth distant from the PZT actuator/sensor is also significant.

Impedance-based health monitoring is a qualitative damage detection method. As in all of the related studies the detailed analysis of modal peaks or frequency shifts in the impedance graphs (Fig. 3.12 - 3.14) is not necessary. The damage for all of the tests is normalized using the Eq. 28. The distant crack test is assigned a value of 100% damage. The remaining tests are compared against this amount of damage (Fig 3.15). The adjacent test revels the frequency dependency of this method. A frequency range that has greater interaction between the PZT and the structure that is above the capacitive nature of the PZT will cause the damage metric to increase. It is important to select a dynamically active frequency range for maximum sensitivity.

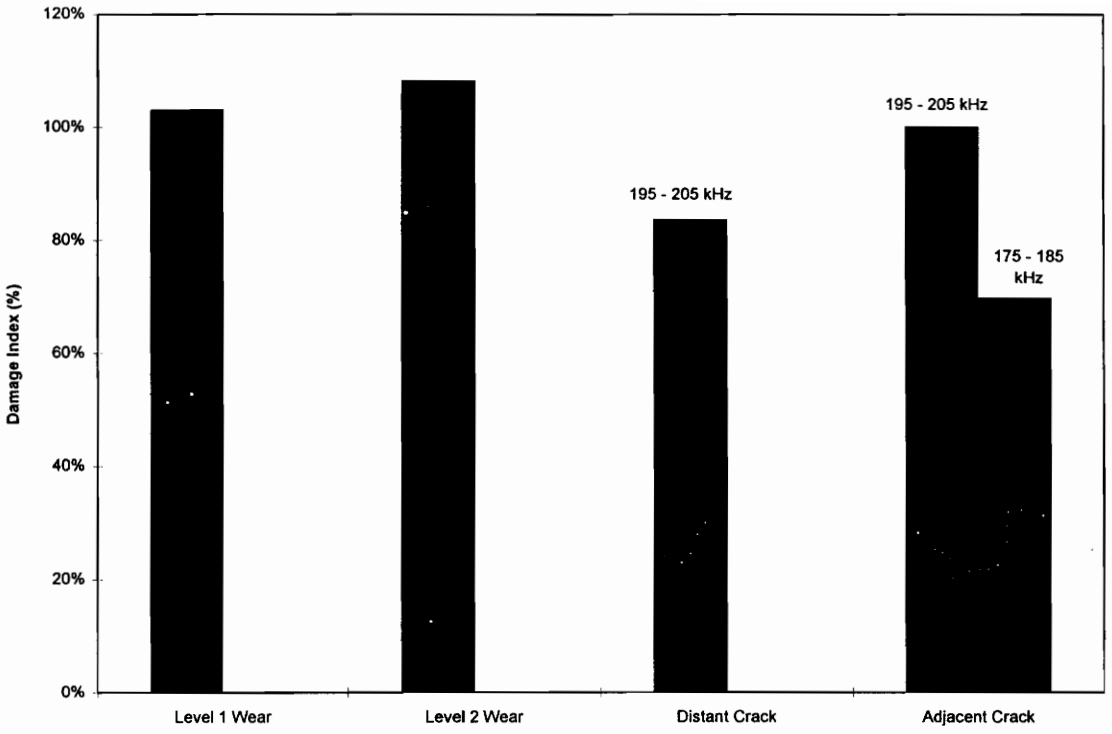

Figure 3.15 The qualitative comparison of the adjacent crack revels the frequency dependency of this health monitoring technique.

Impedance-based health monitoring has been presented as a means to qualitatively monitor incipient damage in complex parts. The chosen high quality gears were subjected to abrasive wear and fatigue cracking. In both cases, the damage was qualitatively detected successfully. In addition, this technique has the potential to be used as a quality assurance technique because of the high repeatability.

3.4 SPACE-BAY TRUSS STRUCTURES

Impedance-based health monitoring can also be used to monitor the structural integrity of space-bay truss structures. This type of structure is smaller, less massive, and considerably lighter than complex civil infrastructure discussed in section 3.6. Nevertheless, there is still a great need for a real-time method for monitoring truss structure integrity.

For this purpose, impedance-based health monitoring is demonstrated on a typical Brussels space frame (Sun et al., 1994) seen in Fig. 3.16. The objective is to qualitatively detect incipient damage within the truss structure and distinguish this local damage from far-field effects of normal use. The localization effect will allow the technique to be sensitive only to local structural changes. Figure 3.16 is a close up picture of a typical Brussels space bay truss structure consisting of pipe members and spherical Delrin balls. Each of the pipe members has a threaded connector at both ends that connects to a Delrin ball. Seven of the Delrin balls (nodes) have a PZT actuator/sensor bonded in a non-intrusive manner. Damage is simulated by tightening or loosening a connector. Because there are several sensing locations, the sensitivity of this technique can be investigated.

Figure 3.17 shows the details of the Delrin ball, pipe connection, and instrumentation setup. PZT actuator/sensor patches (size: 7 x 7 x 0.19 mm) are bonded to the Delrin ball. The frequency range selected for study is 80 kHz - 120 kHz. This range is found to have a high sensitivity with good dynamic action. Several tests are performed on the truss. A local test to observe the effects of local structural changes, and global tests to investigate the effects of far-field damage and the sensitivity of the impedance-based technique.

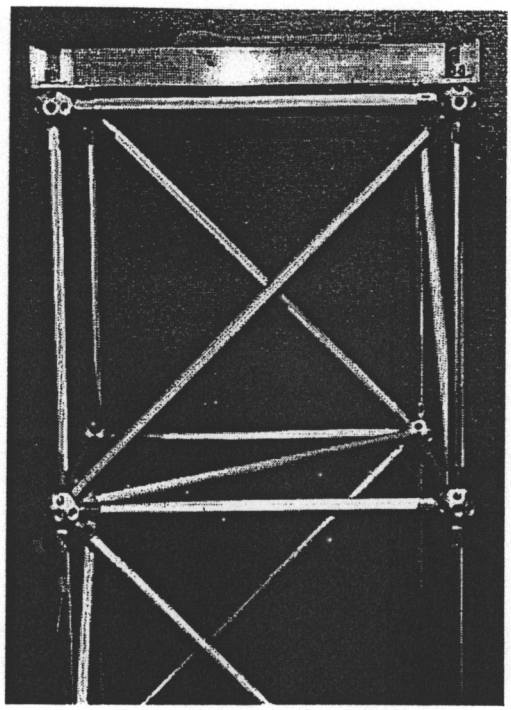

Figure 3.16 Brussels space-bay truss structure with PZT actuator/sensor bonded to a Delrin ball.

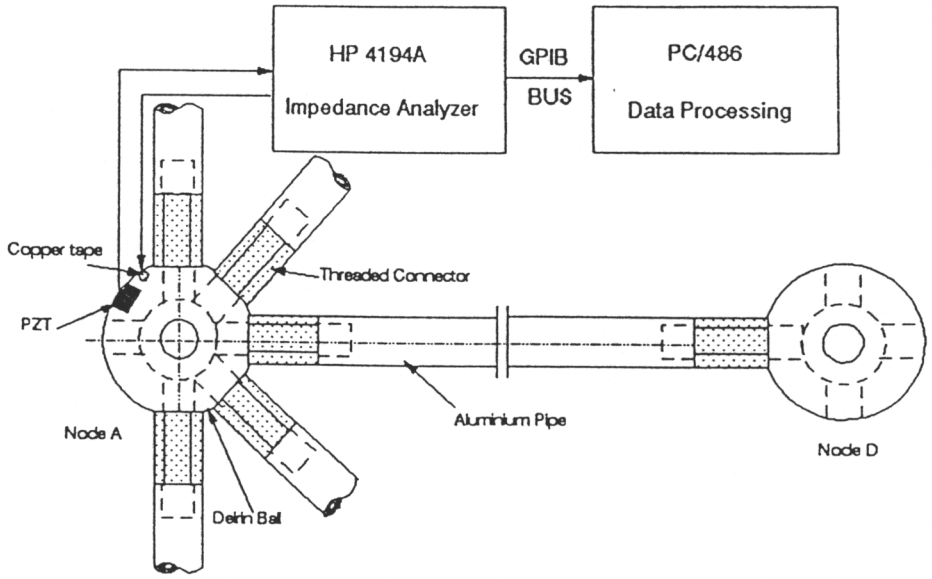

Figure 3.17 Test set-up and instrumentation

The admittance measurements for the local and global damage tests are seen in Fig. 3.18 and 3.19 respectively. The local damage produces clear differences in the trusses resonance's. The admittance patterns are not shifted up or down (as seen later Civil Infrastructure). Nevertheless, the smallest turn of a local joint represents a large change in the admittance measurements.

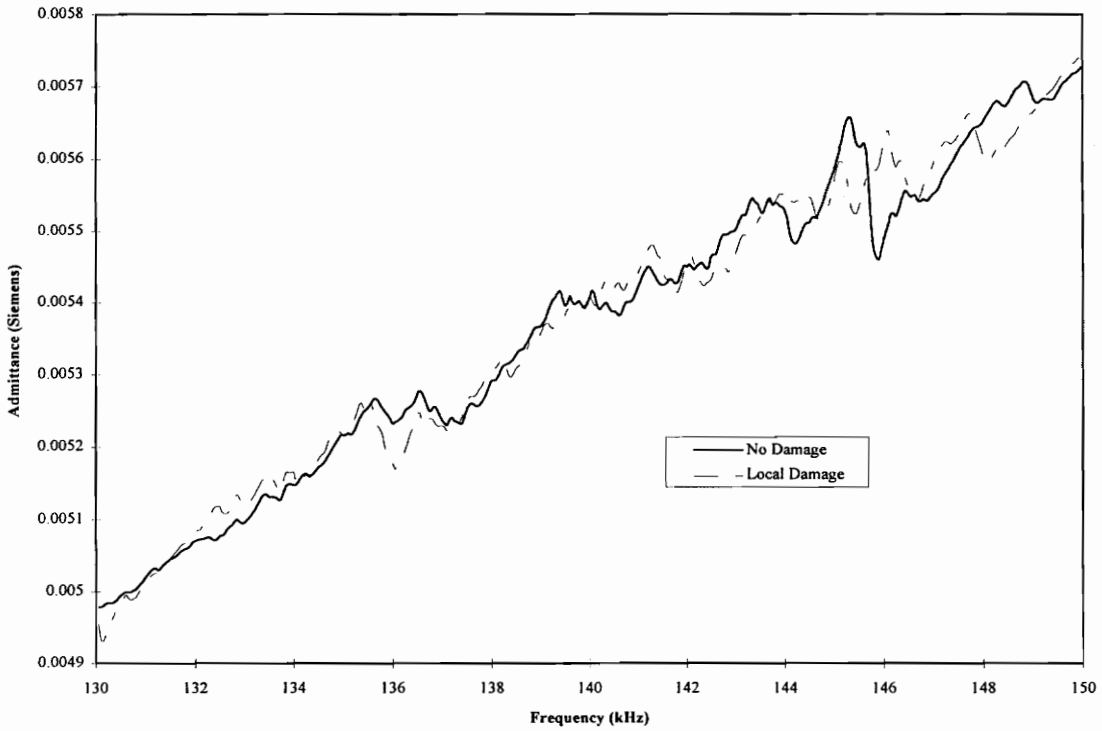

Figure 3.18 Local damage to a space-bay truss structure cause large variations in the admittance measurements.

The impedance-based technique is insensitive to far-field damage. This is displayed in Fig. 3.19. The loosening of a truss connection far from the sensing location has very little effect on the admittance measurements. This is representative of normal usage or normal structural change. There are several factors that contribute to this localization effect; material properties, boundary conditions all effect the degree of the localization effect. However, regardless of the individual structural differences, this phenomena is present in all structures. By placing the PZT actuator/sensor in locations of high stress only the structural changes that represent incipient damage will be detected.

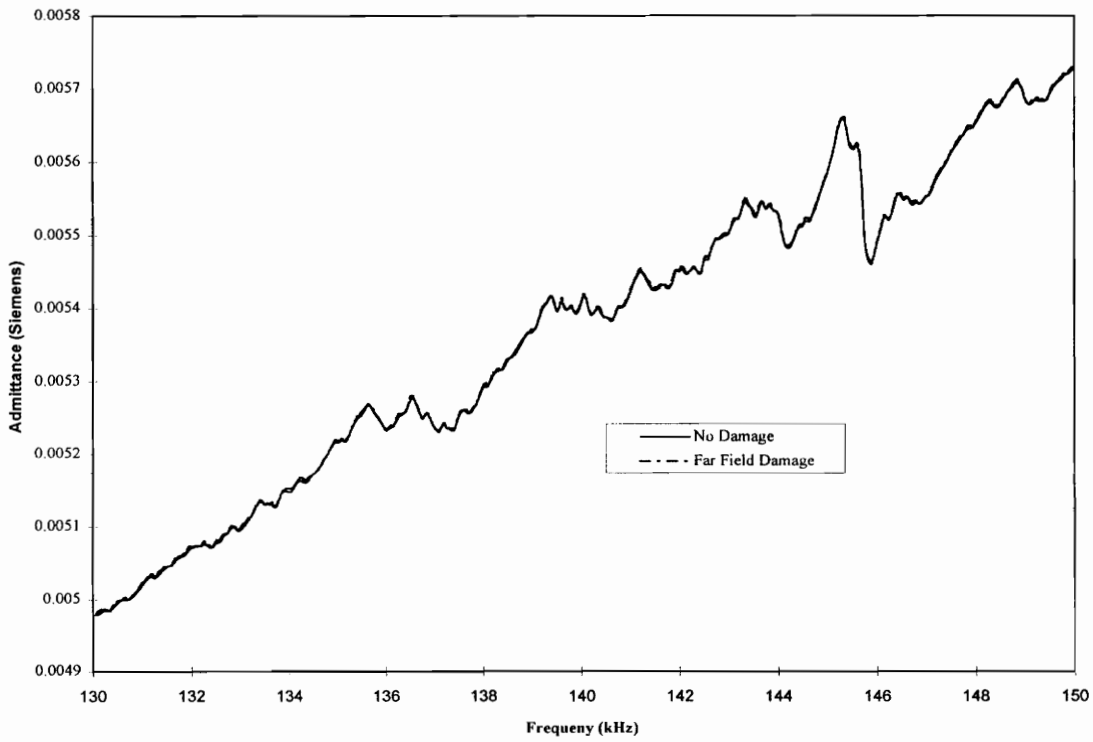

Figure 3.19 Damage that is far from the sensing area has very little effect on the sensing technique.

Equation (28) is used to qualitatively compare the results from the truss structure. This comparison is seen in Fig. 3.20 where the local damage test is assigned a value of 100% damage. A semi-local test is included to further demonstrate the localization effect of this sensing technique. The semi-local test involves loosening a connection between the local and the global sensing areas.

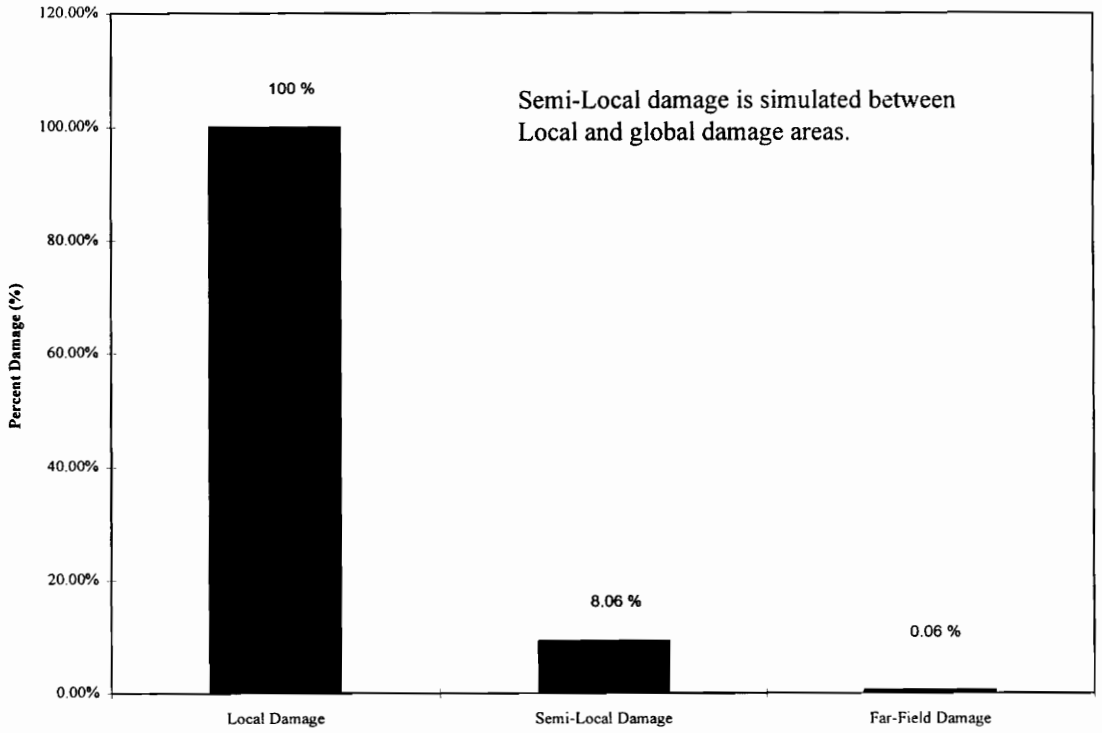

Figure 3.20 Qualitative damage comparison for space-bay truss structures

Impedance-based health monitoring, for the detection of incipient damage in space-bay trusses, has been demonstrated as a feasible qualitative damage detection method. The small size of the PZT actuator/sensors allows for many sensing locations within one structure. In this case study, the localization phenomena was demonstrated. The technique can be facilitated by the use of computers to qualitatively report results.

3.5 AIRCRAFT STRUCTURES

There is a great interest in the aeronautics industry to develop a real-time, in-service health monitoring technique for aircraft structures. The motivation is to reduce the maintenance cost by doing away with the current secluded maintenance inspections. This technique would require an inspections only when incipient damage is detected within the aircraft's structure. Not only would impedance-based health monitoring reduce the aircraft's maintenance cost, it would also lower the planes down time. Currently, when an aircraft is scheduled for a maintenance inspection it must be taken out of service. This health monitoring technique would reduce the time needed to complete the inspections by eliminating certain individual inspections on areas where qualitative health monitoring is used.

Impedance-based health monitoring is tested on a Piper Model 601P aircraft tail-section (Chaudhry et al., 1995). The objective is the monitor the integrity of the two main brackets which connect the rear fuselage to the vertical tail. The actual tail-section used in the experiments is shown in Fig. 3.21. PZT actuator/sensor patches are mounted on the fuselage side of the vertical tail support brackets, each within one inch of the two securing bolts. A close-up view of the tail-section showing the securing bolts and the PZT actuator/sensor is seen in Fig. 3.22. Any alterations in the area of these brackets is considered "local-area" damage.

A number of frequency scans were performed to determine the optimum sensing range for the tail-section. This frequency range is one that contains interaction between the PZT actuator/sensor and the structure that is above the capacitive nature of the PZT. The frequency range selected is 100 kHz - 150 kHz. This range is sensitive to local alterations containing a large quantity of dynamic information about the structure. Two local-area and two far-field (Global) alterations are shown for comparison. The local damage

consisted of the following: loosening one of the bracket bolts 1/8 of a turn, and loosening one of the bracket bolts slightly (the smallest turn possible). The far-field, or global alterations consisted of loosening a bolt far from the sensing area and varying the rudder position.

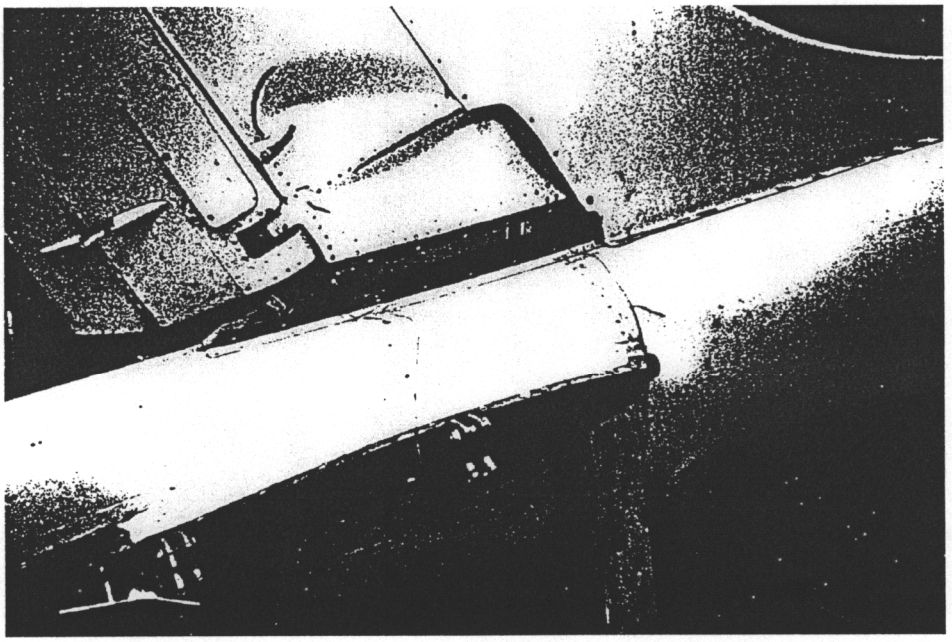

3.21 The tail section of the Piper 601P aircraft used in the case study.

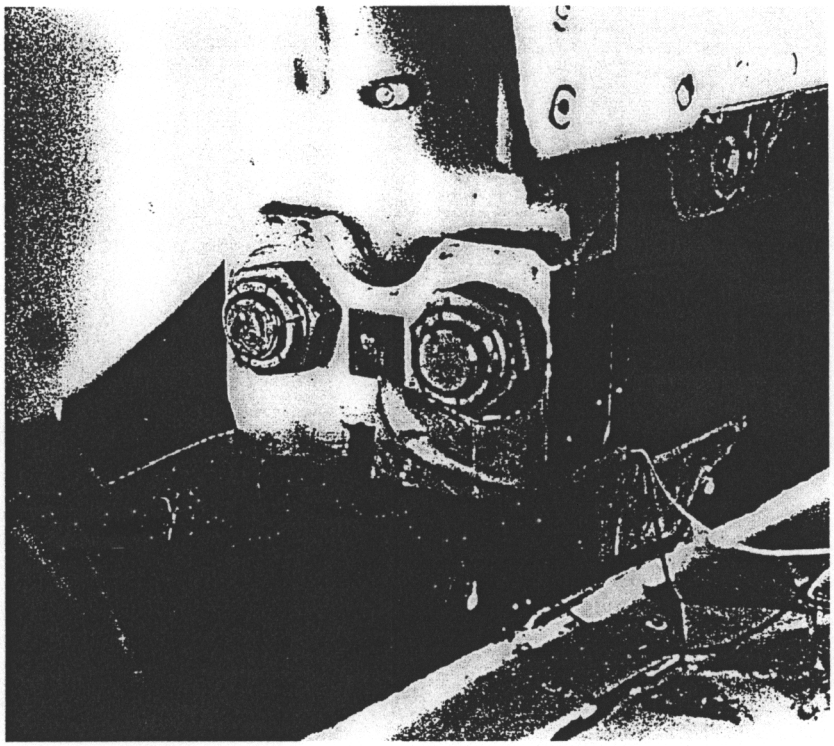

3.22 A close-up view of the vertical tail section support brackets (local-area) showing the bonded PZT actuator/sensor and the bolts used to simulate structural changes.

The local damage admittance measurements, seen in Fig. 3.23 - 3.24, show how sensitive this impedance-based method is to small local structural changes. The smallest amount of local damage results in a change in the admittance pattern. This small structural change results in admittance patterns that are similar. This is due to the fact that the induced damage was so small that the damping properties were not effected. The larger local damage plot seen in Fig. 3.24, has two admittance patterns that much different. The larger bolt turn resulted in an increase in the structural damping. This damping phenomena will be investigated further in the analysis of massive civil infrastructure.

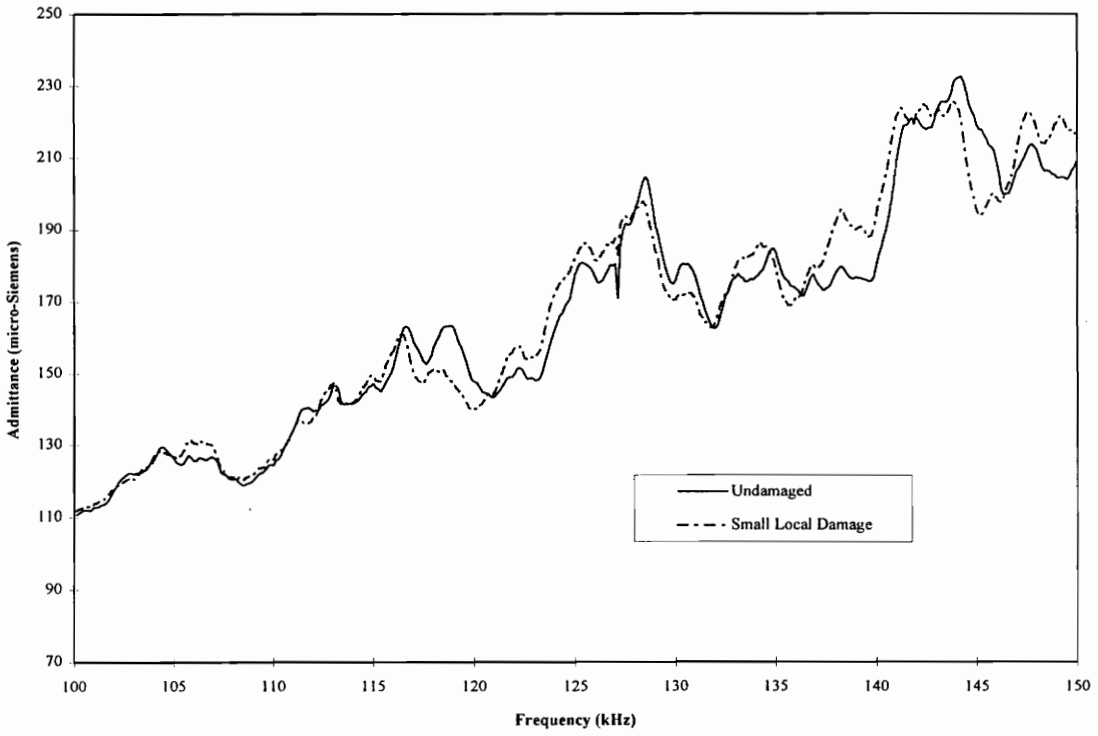

Figure 3.23 The smallest local-area structural alteration results in a change in the admittance measurements.

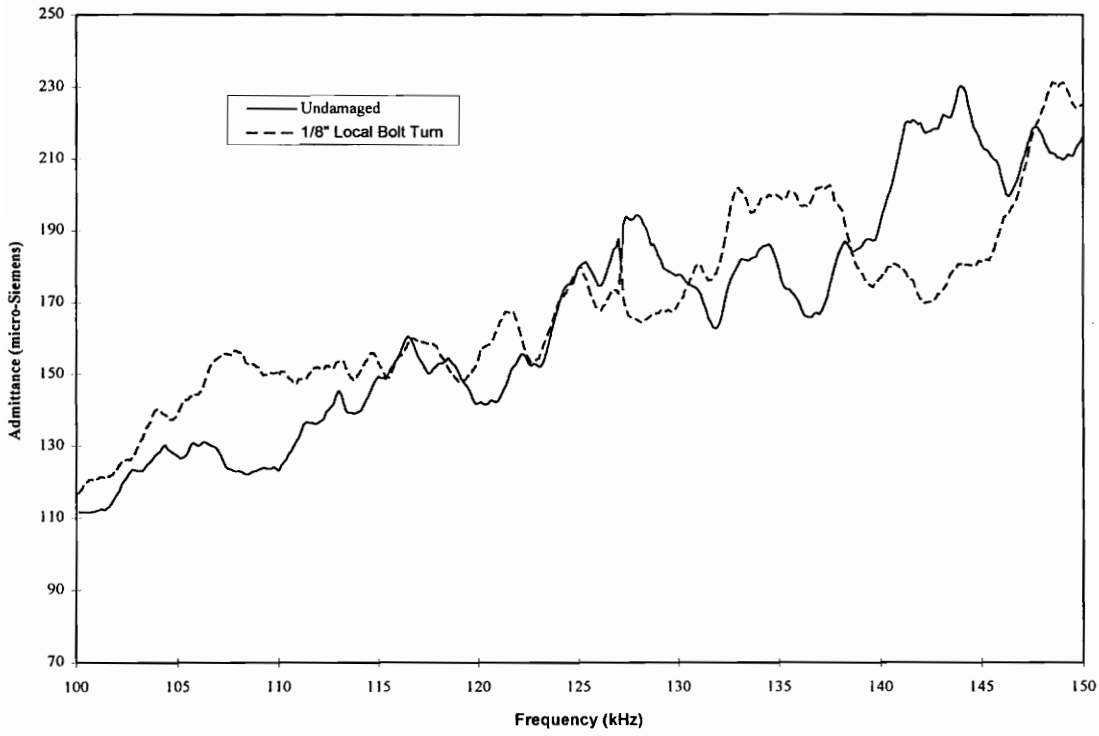

Figure 3.24 Larger structural alteration result in larger differences in the admittance measurements.

The far-field, or global damage admittance measurements, seen in Fig. 3.25 & 3.26, show how insensitive this impedance-based method is to global structural changes. The admittance measurements are almost unchanged due to either global structural alteration. Only the immediate sensing area is affected of the simulated damage. The normal operation, such as rudder changes, would not affect the sensing of the joint.

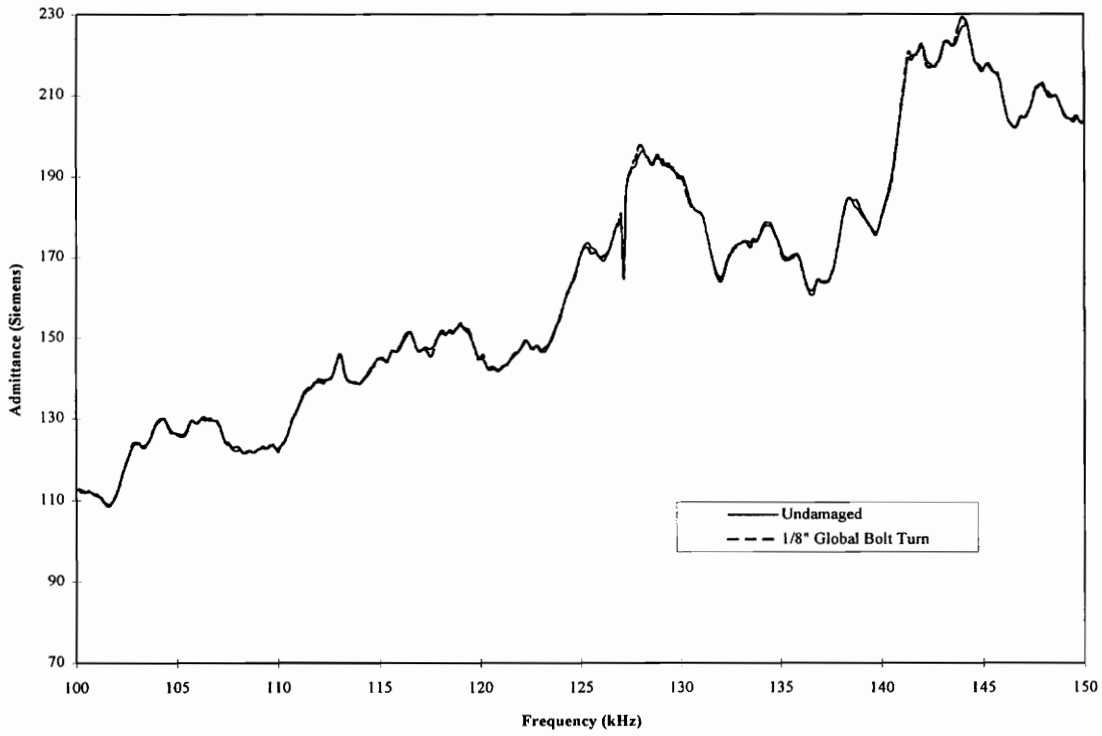

Figure 3.25 The far-field structural alterations have very little impact on this impedance-based sensing technique.

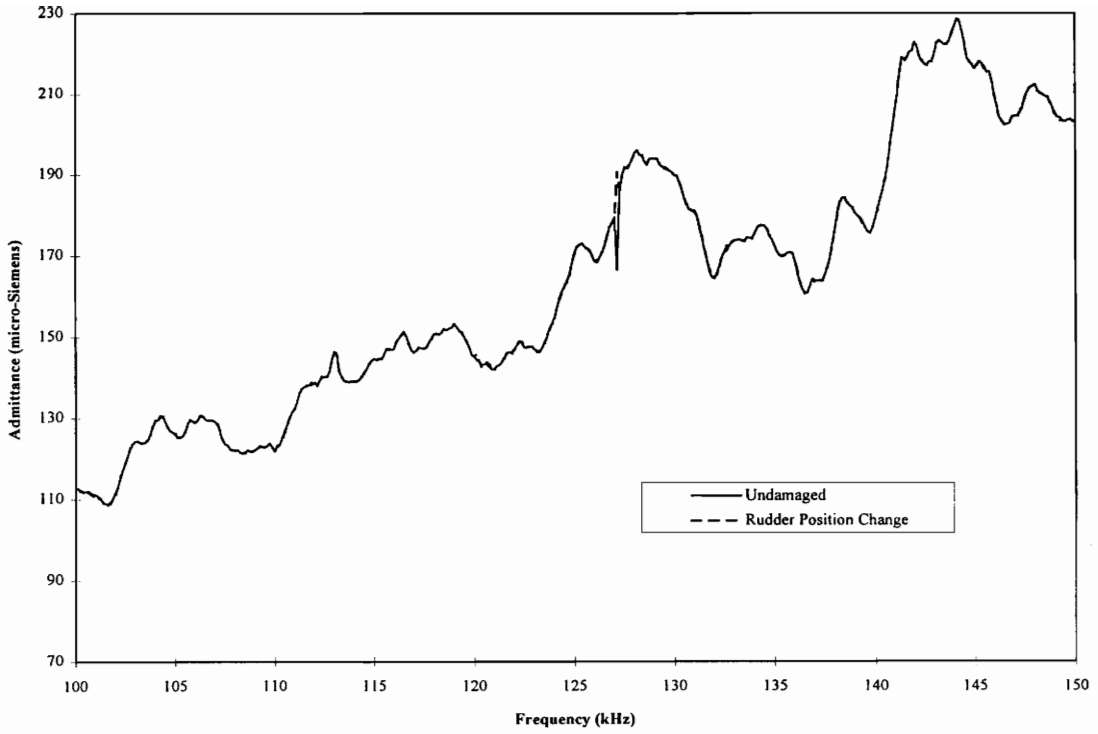

Figure 3.26 Normal operations, such as varying the rudder position, has very little effect on the impedance-based health monitoring technique.

The qualitative comparison for the sensing of aircraft structure can be seen in Fig. 3.27. All of the different tests are normalized using Eq. (28). The 1/8" local bolt test is assigned a damage index of 100%. This qualitative comparison again displays how sensitive this method is to local-area alterations and how global changes have very little effect on the sensing technique.

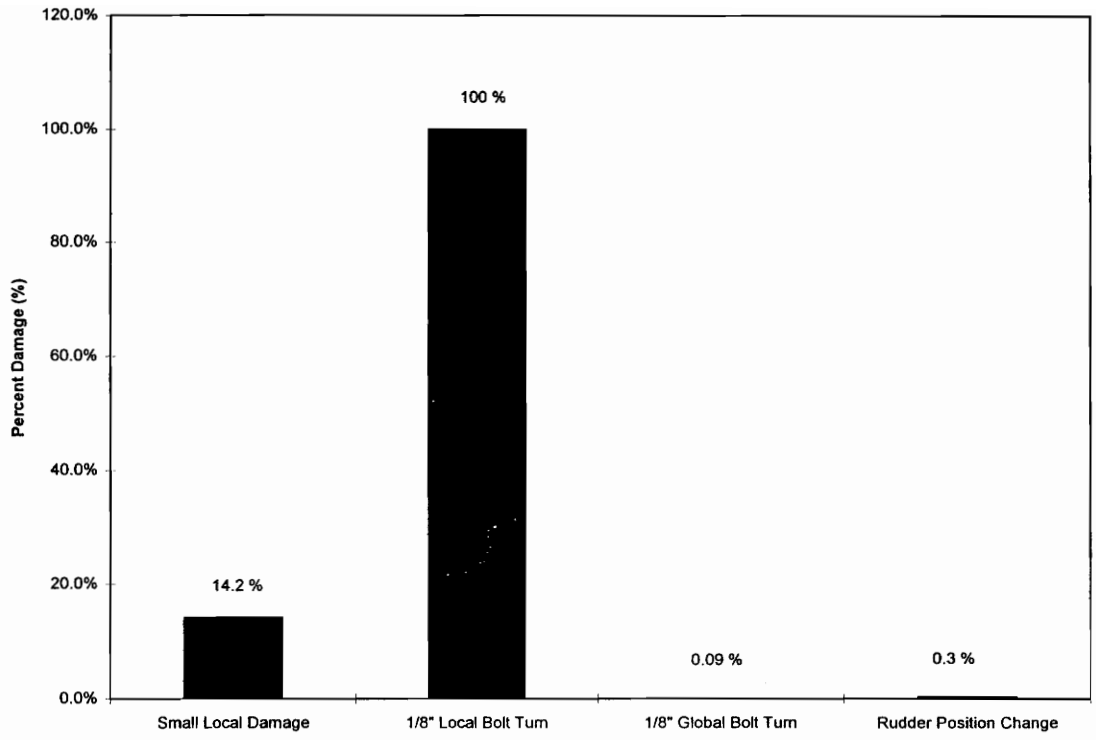

Figure 3.27 The qualitative comparison of the results displays how insensitive this health monitoring technique is to far-field structural alterations.

Impedance-based health monitoring has been demonstrated as a practical means of qualitatively identifying incipient damage in critical areas of aircraft structures, without being affected by the normal operation of the aircraft due to the localized nature of the impedance-based technique.

3.6 CIVIL INFRASTRUCTURE

Today, in the civil engineering community, there is an interest in the development of a real time damage detection method. Bridges require annual inspections that use lots of man power and take months to complete. Over 90% of these annual inspections are unnecessary because nothing is found to be wrong. However, they can not be eliminated because 10% of the time there is something wrong that needs to be fixed. Thus, there is a need for a monitoring technique that is real-time to be used in conjunction with routine maintenance inspections. Many of the structures in the civil engineering world are much larger and massive than any of the structures used in the previous case studies. Thus, there is a need to investigate the effects of this sensing technique on massive structures. The goal of this study is to be able to constantly monitor the integrity of large structures.

A ¼ scale model of a Deck Truss bridge joint is used in the experimental setup. The joint can be seen in Fig. 3.28. The model consists of three W sections, four C channels, four ¼" plates, over 25' of 3X3 angle steel, in excess of 200 bolts, is six feet tall and weights over 500 lb. In the experiments, two PZT actuator/sensor patches are bonded to the joint for the acquisition of the admittance (reciprocal of impedance) over a wide frequency range. Two sensors were bonded due to the large size of the joint. In the admittance measurements only the PZT actuator/sensor closest to the induced damage was used to increase the sensitivity of the impedance variations due to damage. Preliminary tests were performed to determine the optimum frequency range. This range is one that has the most interaction between the PZT sensor and the structure. Interaction is admittance measurements that are above the gradual base line capacitive nature of the PZT. (Large peaks and valleys) For this bridge joint the best range is 350-370 kHz.

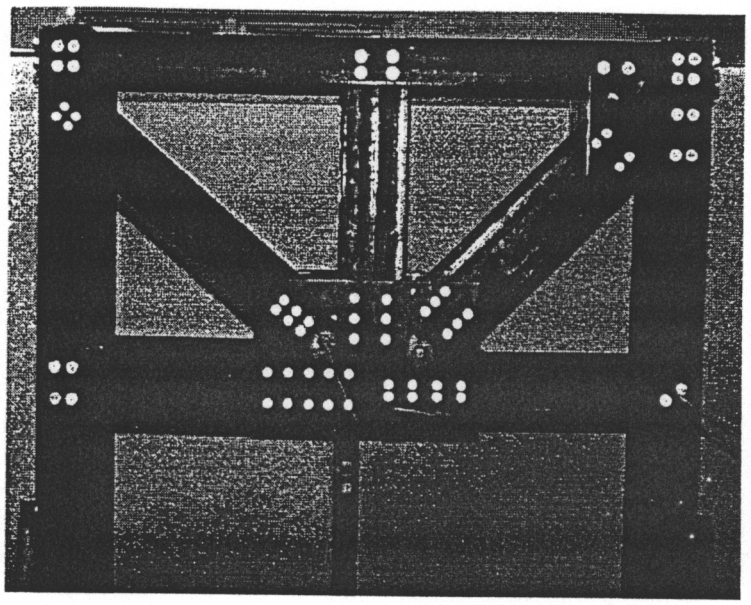

Figure 3.28 The bridge joint and support structure used in the experiments.

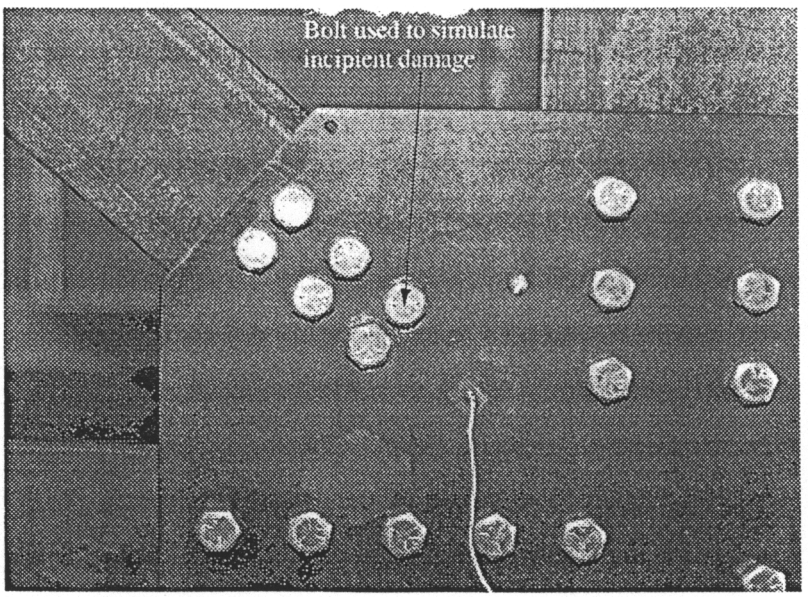

Figure 3.29 A close-up of the bridge joint showing the bolts used to simulate local damage and the PZT actuator/sensors.

Damage is simulated in the joint by loosening bolts in the structure. Two types of damage are simulated, local and global. Local damage is damage that is close to the PZT actuator/sensor, representative of actual incipient joint damage. Global damage is far from the sensing area and is representative of normal usage of the bridge such as traffic passing over the bridge. For the local damage, four levels of damage were simulated by loosing 1, 2, 6, and 14 bolts in the vicinity of the PZT actuator/sensor. For the global damage, one of the four bolts in the upper left corner of the structure is loosened. In each of these tests the bolt (s) is loosened ½ turn. A single bolt loosened ½ turn is representative of incipient damage since the integrity of the joint is still maintained.

The admittance measurements for the two types of damage, global and local, are presented for visual comparison and verification of the method. The global damage test (Fig 3.30) shows how the impedance-based method is insensitive to far field damage. The admittance measurement is almost unchanged with the global damage. This is a phenomena that occurs regardless of the selected frequency range. A frequency range that is less sensitive will produce an even smaller change in the measurements. The local damage tests reveal several aspects of this method. The one-bolt damage test (Fig. 2.31) produced a small vertical shift in the admittance measurements. This shows how sensitive this damage detection method is to incipient damage in the sensing area. When the local damage is increased by loosing two bolts, a larger vertical shift is seen in the admittance measurements (Fig. 2.32). Also, a small variation in the peaks and valleys starts to appear. This vertical shift is representative of the stiffness of the structure and the lack of damping at the sensing location. Small amounts of damage will show up as an admittance vertical shift. For structures that are not very stiff or with a greater internal material damping, such as the aircraft fuselage, even small amounts of local damage will produce a significant change in the admittance measurements. Finally, a large amount of local damage (Fig. 3.33) will cause a distinct change in the admittance measurements. This distinct change occurs because the large damage modifies the apparent stiffness of the

joint, which was not the case for the incipient damage (one bolt test). As for the previous work on various proof-of-concept demonstrators, the localization effect and the ability to detect incipient damage is maintained.

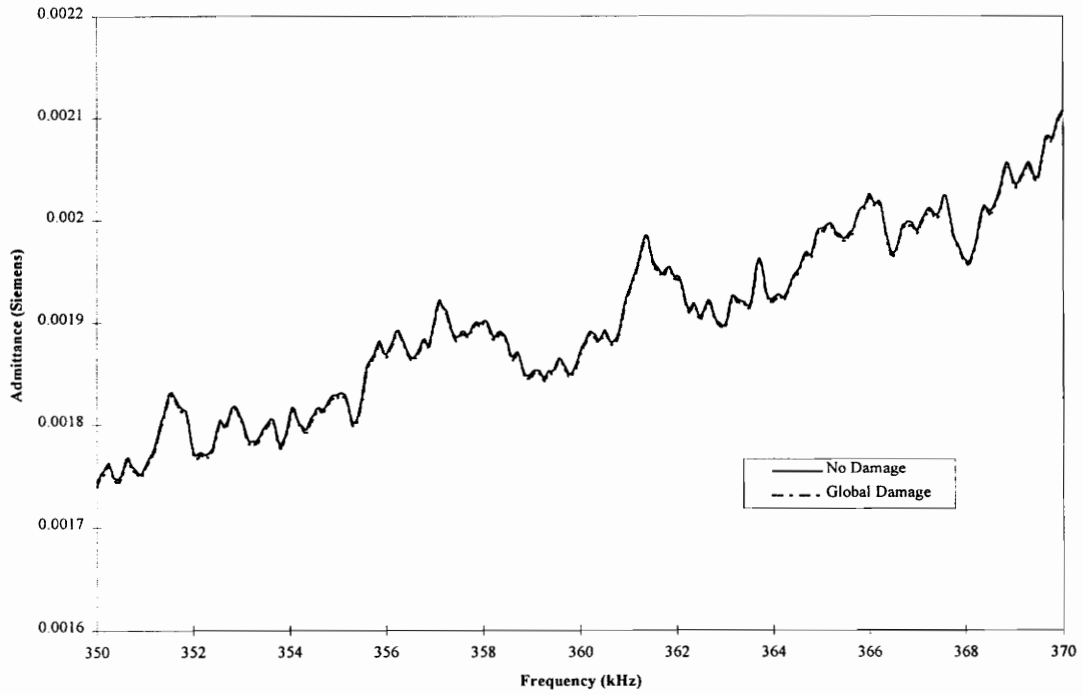

Figure 3.30 The local sensing area is insensitive to global structural alterations.

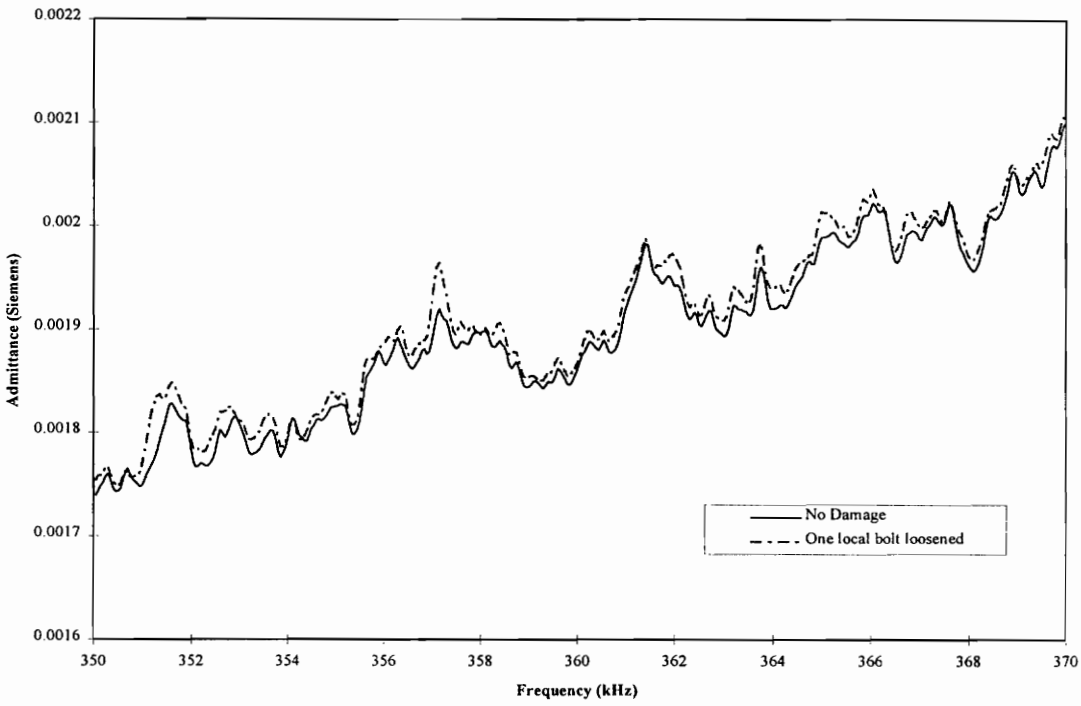

Figure 3.31 The local sensing area is very sensitive to the smallest amount of local structural alterations.

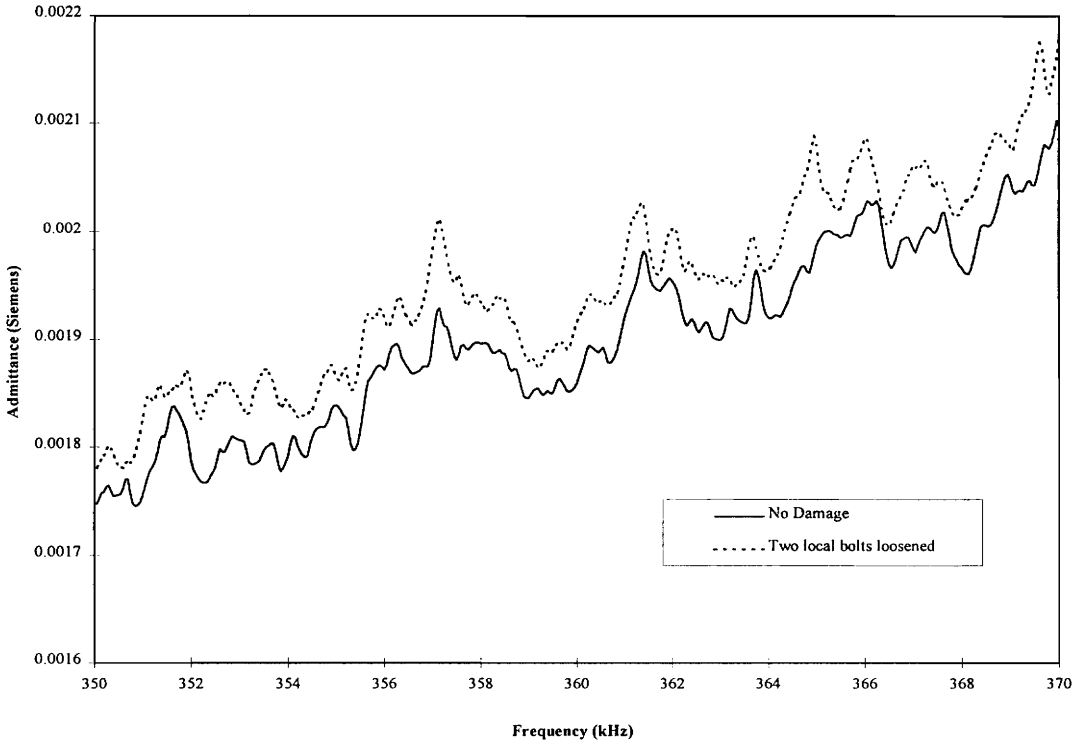

Figure 3.32 Small amounts of local damage produce vertical shifts in the admittance measurements.

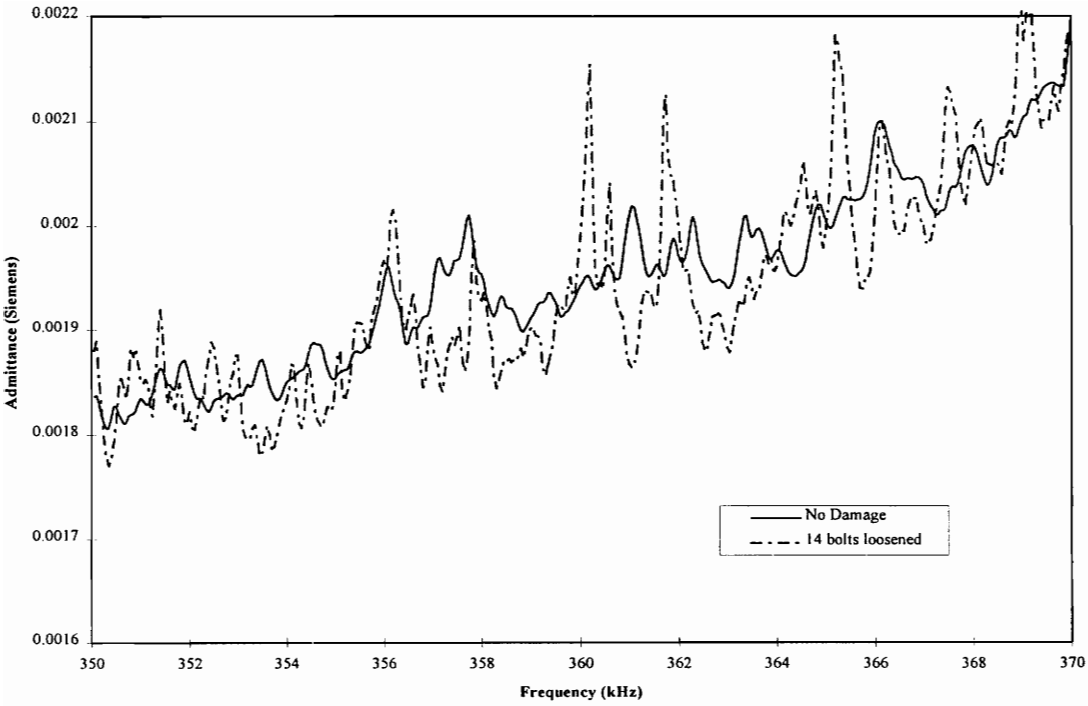

Figure 3.33 Large local structural alterations cause large variations in the admittance measurements.

Equation (28) is used to quantify the different tests. This damage metric is then normalized by choosing an arbitrary amount of damage (such as the two bolt damage) and assigning this damage a value of 100%; all other measurement are then compared to this known amount.

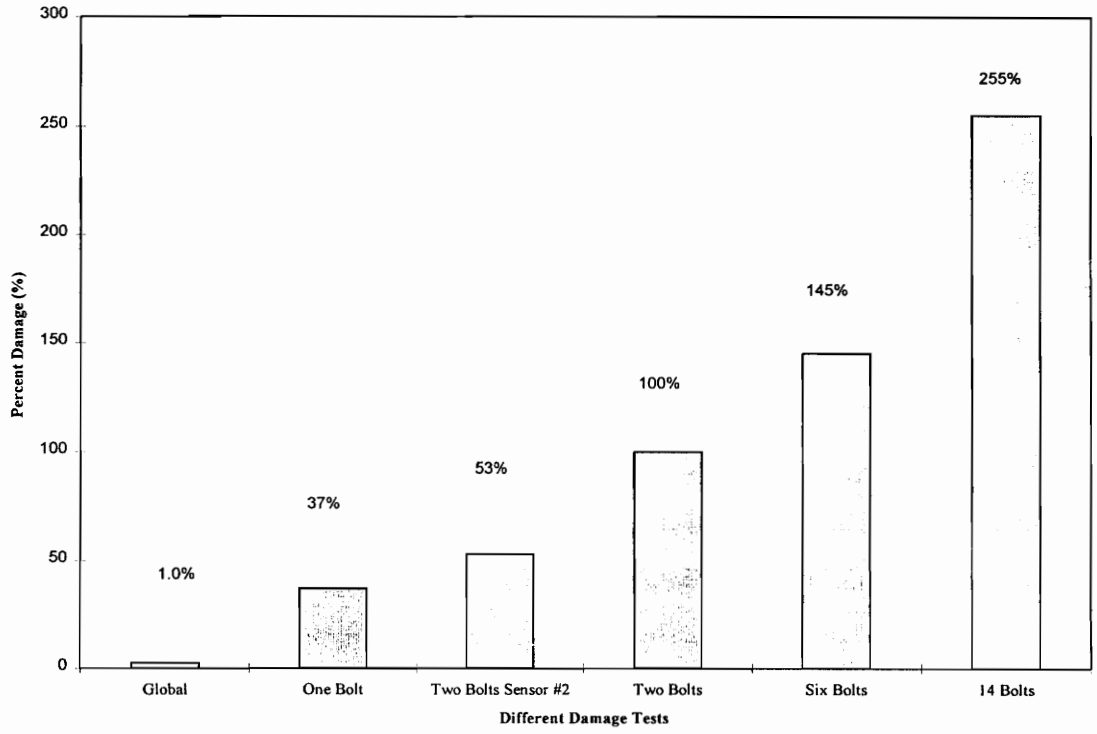

Figure 3.34 A qualitative comparison shows the impedance-based techniques sensitivity to local and global damage.

The impedance-based technique is able to find incipient damage on a joint and distinguish it from normal usage of the joint due to the localization effect. The damage metric of global damage and four levels of local damage is presented in Fig. 3.34. The global metric is many times less than (less than 2% actual damage) the value of the one local bolt test. This small value indicates the insensitivity of the sensor to far-field disturbance. This localization effect can also be seen in the two bolt test using sensor

number two. This PZT sensor is located on the plate that the damage occurs, however, it is further from the induced damage than sensor number 1. This translates into less perceived damage and indicates that large structures may need more than one sensor/actuator at any critical location. The impedance-based technique is a qualitative technique, that is it can not determine if the damage is due to cracks, corrosion, de-bonds, or loose connections. However, the technique is somehow quantitative, showing an increasing damage metric with increasing local damage; as it can be seen in figure 3.34. The damage metric can give some indication on the level of damage when compared to the known reference damage (two bolt test). A damage metric larger than 100% indicates more damage than the reference damage. To further simplify the interpretation of the results, a computer can be used to compare many different locations and report the results only when a threshold value is reached. This report can be in the form of a red light or a siren on a control panel far from the actual sensing location.

The impedance-based health monitoring technique is a real-time structural damage detection method that has been successfully demonstrated on a massive bridge joint. It utilizes the change in coupled electro-mechanical impedance of a bonded piezoelectric actuator/sensor as the means to qualitatively detect structural damage and actively monitor a structures integrity. This technique, because of the high frequencies of operation, is very sensitive to damage local to the sensing area.

CHAPTER 4

4.1 DISCUSSION

The implementation of the impedance-based qualitative health monitoring technique can be made easier by the use of computers and micro circuits. Many damage detection methods require background knowledge of the technique in order to interpret the output. One strength of the impedance-based health monitoring technique is that it can be implemented so that anyone can interpret the results through the simple damage metric. The ultimate scope of non-destructive evaluation is to implement the method on a structure and then to receive the output at a remote location in real-time. The output at this remote location should be easy to interpret, such as a red light on a multipurpose control panel. The impedance-based health monitoring technique has the ability to monitor many different sensing locations on a structure because of the localization effect, and these locations can all be monitored at the same control panel. Several different structures can also be monitored at the same control station. There is no limit to the number of sensing locations. Computer algorithms can be written to connect small or large amounts of sensors to one location. The feasibility of wide spread real-time integrity monitoring of structures becomes closer to a reality with this qualitative technique. This method has great potential in the engineering community to reduce the maintenance cost of existing structures. It also has the potential, in the future, to enable engineers to design systems and structures with less over-engineering.

4.2 FUTURE ISSUES

There are certain issues that still need further investigation before a full-scale implementation of the impedance-based NDE technique can take place. Included in these issues is the temperature stability of the electrical properties for the piezoelectric material. Currently, the method directly measures the electrical properties and any change in the electrical properties that is associated with a change in temperature can be confused as damage. This is an important problem since large temperature variations are common in real-life applications. However, this issue is currently under investigation at CIMSS. A computer algorithm under development will incorporate the temperature effects into all health monitoring applications. (Kirshnamurthy et al., 1996) The last major issue that needs to be investigated is the software that support this technique. A computer code that will tie all of the individual algorithms together is needed. These algorithms include: acquisition of the data, qualitatively preparing the data, correction of temperature effects, and sending a damaged or un-damaged single to the control panel.

4.3 CONCLUSIONS

The impedance-based health monitoring technique presented in this thesis is a real-time damage detection method that was proven to be able to qualitatively detect incipient damage in a wide variety of structures. In the first case study presented, composite patch repair, it is able to detect the smallest de-bond between the host structure and the patch. Impedance-based health monitoring has also been shown successful in determining failures in complex precision parts. Each of the high quality gears were subjected to abrasive wear or fatigue due to bending cracks. In each case the damage was qualitatively detected. It was also shown that this method can be used as a quality control device by comparing the similarities in the admittance measurements for each precision part. The

impedance-based technique was shown successful in detecting incipient damage in a space-bay truss. This was the first demonstration of the technique's localization phenomena. This phenomena allows only structural alterations that are in the immediate sensing area to be detected. Structural changes in an aircraft structure were easily detected by this impedance-based health monitoring technique. Again, the insensitivity of far-field structural alterations was seen by varying the aircraft's rudder position. Impedance-based health monitoring was finally demonstrated successfully on massive bridge joint. In summary, the impedance-based NDE technique has been shown successful on a variety of structures. All of the case studies show that the impedance-based technique very robust in field applications.

REFERENCES

Alban, L.E., 1985, "Systematic Analysis of Gear Failures," ASM publishing, OH.

Baker, D.K., 1989, **Active Dynamic Response Tuning of Adaptive Composites Utilizing Embedded Nitonal Actuators**, Masters Thesis, Virginia Polytechnic Institute and State University.

Cawley, P., 1987, "The Sensitivity of the Mechanical Impedance Method of Non-destructive Testing," *NDT International*, Vol. 20, pp. 209-215.

Cawley, P., and Adams, R.D., 1988 "The Mechanics of the Coin-tap Method of Non-destructive Testing," *Journal of Sound and Vibration*, Vol. 122, pp.299-316.

Cawley, P., and Theodorakopoulos, C., 1989, "The Membrane Resonance Method of Non-destructive Testing," *Journal of Sound and Vibration*, Vol. 130, pp.299-311.

Chaudhry, Z., Lalande, F., Ganino, A., Rogers, C.A., and Chung, J., 1995b, "Monitoring the Integrity of Composite Patch Structural Repair via Piezoelectric Actuators/Sensors," *Proceedings*, AIAA/ASME/ASCE/ASH/ASC 36th Structures, Structural Dynamics, and Materials Conference, New Orleans, LA, April 11-14, 1995, pp. 2243-2248.

Chaudhry, Z., Joseph, T., Sun, F., and Rogers, C.A., 1995a, "Local-area Health Monitoring of Aircraft via Piezoelectric Actuator/Sensor Patches," *Proceedings*, SPIE 1995 North American Conference on Smart Structures and Materials, San Diego, CA, SPIE publishing, Bellingham, WA, Vol. 2443, pp. 268-276.

Chung, J.H., 1993, "Cost Effective Aircraft Repair: Composite Repair of Aircraft Structure," *Proceedings*, Defense Manufacturing Conference, Vol. II, San Francisco, CA, pp. 551-574.

Guyott, C.C.H., Cawley, P., and Adams, R.D., 1986, "The Non-Destructive Testing of Adhesively Bonded Structure: A Review," Journal of Adhesion, Vol. 20 pp. 129-159.

Krishnamurthy, K., Chaudhry, Z., Lalande, F., and Rogers, C.A., 1996, "Effects of Temperature on the Electrical Impedance of Piezoelectric Sensors," *Proceedings*, SPIE North American Conference on Smart Structures and Materials, San Diego, CA, SPIE publishing, Bellingham, WA; in press.

Lalande. F., Childs, B., Chaudhry, Z., and Rogers, C.A., 1996, "Frequency Impedance for NDE of Complex Precision Parts," *Proceedings*, SPIE North American Conference on

Smart Structures and Materials, San Diego, CA, SPIE publishing, Bellingham, WA; in press.

Liang, C., Sun, F.P., and Rogers, C.A., 1994, "Coupled Electromechanical analysis of adaptive material - Determination of the power consumption and system energy transfer," Journal of Intelligent Material Systems and Structures, Vol. 5, No. 1, January 1994, pp. 21-20.

Liang, C., Sun, F.P., and Rogers, C.A., 1993, "An impedance Method for Dynamic Analysis of Active Material Systems," *Proceedings*, AIAA/ASME/ASCE/ASH/ASC 35th Structures, Structural Dynamics, and Materials Conference, La Jolla, CA, pp. 3587-3599.

Rogers, C.A., "Intelligent Material Systems - the Dawn of a New Materials Age," *Science of Machine Journal*, Vol. 46, No. 9, pp. 977-983.

Rogers, C.A., 1994, "The Impedance Method for Understanding Energy Transfer and Power Consumption Issues In Smart Structures," *Proceedings*, 34th Israel Conference on Aerospace Sciences, February, 1994, Tel Aviv, Israel.

Sun. F., Liang. C., and Rogers. C.A., 1995, "Structural Frequency Response Function Acquisition via Electric Impedance Measurement of Surface-Bonded Piezoelectric Sensor/Actuator," *Proceedings*, AIAA/ASME/ASCE/ASH/ASC 36th Structures, Structural Dynamics, and Materials Conference, New Orleans, LA, AIAA Publishing, Washington, DC, April 11-14, 1995, pp. 3450-3458.

Sun, F., Chaudhry, Z., Liang, C., and Rogers, C.A., 1994, "Truss Structure Integrity Identification Using PZT Sensor-Actuator," *Proceedings*, Second International Conference on Intelligent Materials, Williamsburg, VA, 5-8 June, 1994; pp. 1210-1222.

VITA

John W. Ayres III was born on April 26, 1971, in Richmond, Virginia. He attended Midlothian High School for two years before transferring to Fork Union Military Academy in 1988 where he graduated in May 1990. From there he entered the Virginia Military Institute in pursuit of a B.S. degree in Mechanical Engineering. After the completion of his undergraduate work in 1994 he decided to continue his academic experience and entered the Virginia Polytechnic Institute and State University for a M.S. in Mechanical Engineering.
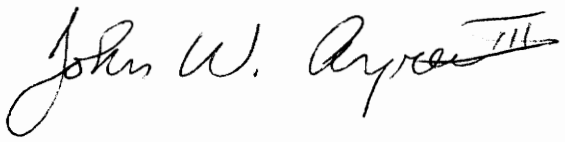
Upon the complication of his Masters degree he will begin a career with Lucent Technologies Bell Labs Innovation (formerly AT&T Power Systems) in Dallas Texas.